Available online at www.sciencedirect.com
SCIENCE DIRECT
Precambrian Research 146 (2006) 45–67
Precambrian Research
www.elsevier.com/locate/precamres

Zircon geochronology and metamorphic evolution of mafic dykes in the Hengshan Complex of northern China: Evidence for late Palaeoproterozoic extension and subsequent high-pressure metamorphism in the North China Craton

A. Kröner[a,*], S.A. Wilde[b], G.C. Zhao[c], P.J. O'Brien[d], M. Sun[c], D.Y. Liu[e], Y.S. Wan[e], S.W. Liu[f], J.H. Guo[g]

[a] *Institut für Geowissenschaften, Universität Mainz, D-55099 Mainz, Germany*
[b] *School of Applied Geology, Curtin University of Technology, GPO Box U1987, Perth, WA 6845, Australia*
[c] *Institut für Geowissenschaften, Universität Potsdam, Postfach 601553, D-01553 Potsdam, Germany*
[d] *Department of Earth Sciences, University of Hong Kong, Pokfulam Road, Hong Kong, China*
[e] *SHRIMP Isotope Laboratory, Chinese Academy of Geological Sciences, 26 Baiwanzhuang Road, Beijing 100037, China*
[f] *School of Earth and Space Sciences, Peking University, Beijing 100871, China*
[g] *Institute of Geology & Geophysics, Chinese Academy of Sciences, Beijing 100029, China*

Received 22 December 2004; received in revised form 20 December 2005; accepted 12 January 2006

Abstract

Magmatic and metamorphic zircons have been dated from ductilely deformed gabbroic dykes defining a dyke swarm and signifying crustal extension in the northern part of the Hengshan Complex of the North China Craton. These dykes now occur as boudins and deformed sheets within migmatitic tonalitic, trondhjemitic, granodioritic and granitic gneisses and are conspicuous due to relics of high-pressure granulite or even former eclogite facies garnet + pyroxene-bearing assemblages. SHRIMP ages for magmatic zircons from two dykes reflect the time of dyke emplacement at ~1915 Ma, whereas metamorphic zircons dated by both SHRIMP and evaporation techniques are consistently in the range 1848–1888 Ma. The youngest granitoid gneiss yet dated in the Hengshan has an emplacement age of 1872 ± 17 Ma. These results complement recent geochronological studies from the neighbouring Wutai and Fuping Complexes, to the SE of the Hengshan, showing that a crustal extension event occurred in the late Palaeoproterozoic. This preceded a major high-pressure collision-type metamorphic event in the central part of the North China Craton that occurred in the Palaeoproterozoic and not in the late Archaean as previously thought. Our data support recent suggestions that the North China Craton experienced a major, craton-wide orogenic event in the late Palaeoproterozoic after which it became cratonized and acted as a stable block.

Keywords: Hengshan; Mafic dyke; Metamorphism; North China Craton; Palaeoproterozoic; Zircon geochronology

1. Introduction

The evolution of Archaean to Palaeoproterozoic rocks in the North China Craton (NCC; also known as the Sino-Korean Craton) has been the subject of widespread interest, as well as controversy, in recent years. As plate

* Corresponding author. Tel.: +49 6131 3922163; fax: +49 6131 3924769.
E-mail address: kroener@mail.uni-mainz.de (A. Kröner).

0301-9268/$ – see front matter © 2006 Elsevier B.V. All rights reserved.
doi:10.1016/j.precamres.2006.01.008

tectonic models have been developed to explain the episodes of magmatism, metamorphism and sedimentation it has been necessary to establish the age and duration of these processes in order to test and validate the models. Well established in the Chinese literature are the Qianxi (>3.0 Ga), Fuping (3.0–2.5 Ga), Wutai (2.5–2.4 Ga) and Lüliang (2.4–1.8 Ga) cycles (Huang, 1977; Liu et al., 1985, 1990; Ma et al., 1987; Wang and Mo, 1995). These names are now used for supposed tectono-metamorphic events which, in more recent models, mark the end points of these cycles. It is now generally agreed that the NCC is an amalgamation of different nuclei which collided during the late Archaean and Palaeoproterozoic. The discovery of rocks interpreted as belonging to ancient island arc or oceanic crust domains, as well as rare findings of rocks usually associated with modern subduction-collision zones (high-pressure granulites, eclogites, calc-alkaline granitoids), has strengthened the block collision models (e.g. Zhai et al., 1993, 1995; Zhao et al., 2001a, 2005; Guo et al., 1996, 2002; Li et al., 2002; O'Brien et al., 2005; Kröner et al., 2005a,b). However, interpretations of the number of blocks, their regional extent, and the age of magmatic and metamorphic events in and between the various blocks remain

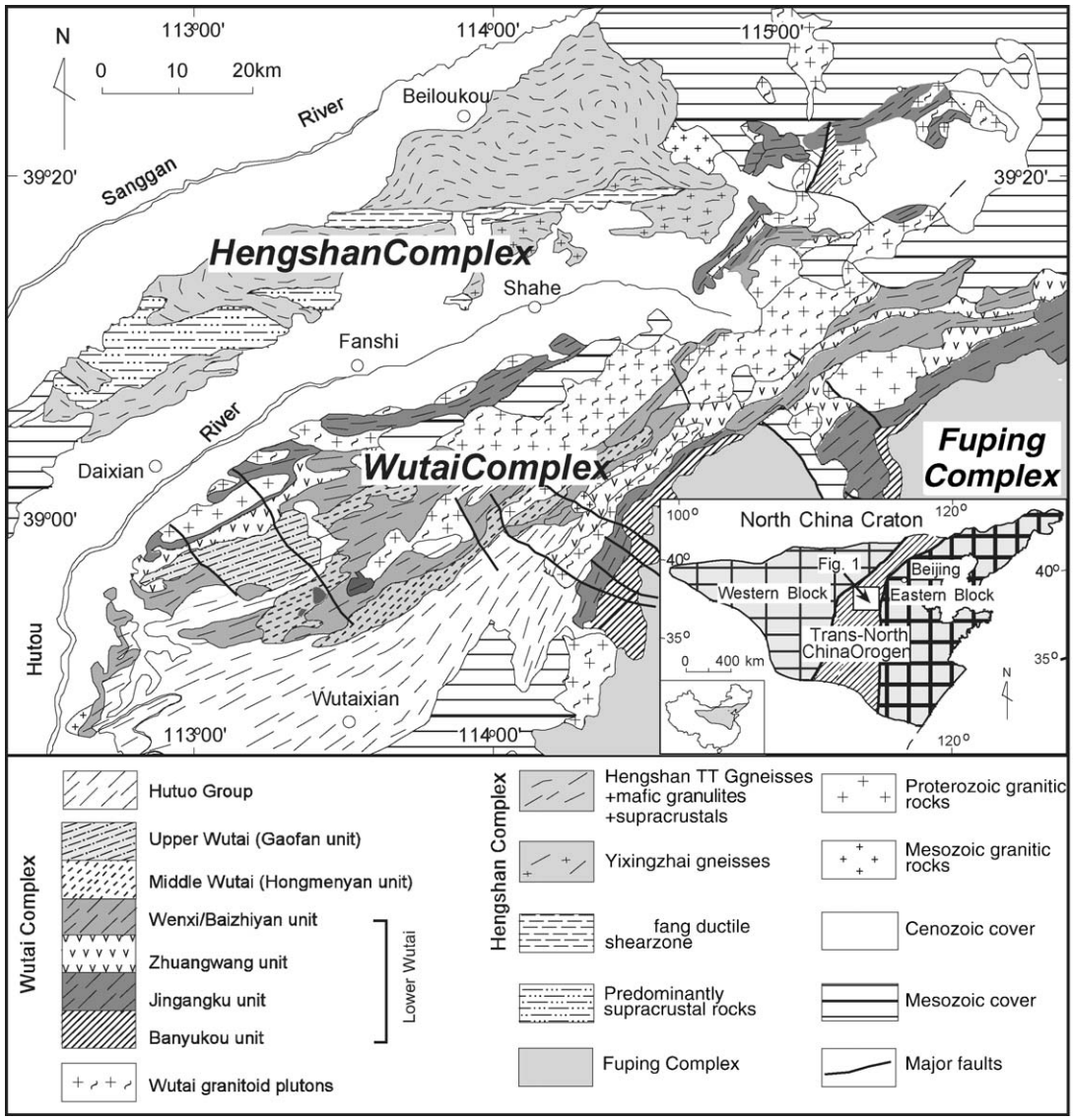

Fig. 1. Simplified geological map of the Hengshan–Wutaishan–Fuping area showing major rock units (modified after Zhao et al., 1999c). Inset in lower right corner shows North China Craton with Eastern and Western Blocks and Trans-North China Orogen (from Zhao et al., 2002a,b). Location of study area is also indicated.

controversial. One of the reasons for disagreement is the contrasting interpretation of isotopic data by different authors. The available Nd model ages, isochrons and errorchrons, concordia upper and lower intercept ages, and cooling ages have all been selectively used in the various attempts to interpret the magmatic and metamorphic history of the region. Essentially, major disagreement still exists as to whether block collision, high-pressure metamorphism, and craton consolidation is of Palaeoproterozoic (ca. 1.85–1.9 Ga; Zhao et al., 2002b, 2005; Guan et al., 2002; Guo et al., 2005; Wang et al., 2003; Kröner et al., 2005a,b) or late Archaean age (ca. 2.5 Ga; e.g. Li and Qian, 1994; Tian et al., 1996; Li et al., 2000a,b; Kusky and Li, 2003).

In a series of recent papers (Wilde et al., 1997, 1998, 2004; Zhao, 2001; Zhao et al., 1998, 1999a, 2000a, 2002b, 2005) evaluation of characteristic lithological, structural, metamorphic and geochronological features of the exposed Precambrian crystalline complexes has led to the hypothesis of a Palaeoproterozoic continental collision belt, the Central Zone (also named the Trans-North China Orogen, Zhao et al., 1999a), located between the Eastern and Western Blocks (Fig. 1). The zones are separated by major faults, and within each block there are also several fault-bounded terranes. One of the features used to characterize the different blocks was the difference in style of granulite-facies metamorphism of mafic rocks. Both medium-pressure (MP) and high-pressure (HP) mafic granulites exist (e.g. Jin and Li, 1996; Zhao et al., 1999a). The HP-granulites, containing clinopyroxene and garnet, formed above 10 kbar and show secondary orthopyroxene due to near-isothermal decompression pressure–temperature (*P–T*) paths (Wang et al., 1991; Zhai et al., 1993; Lu and Jin, 1993; Liu, 1996; Li et al., 1998a,b; Zhao et al., 2000a,b, 2001a,b; Guo et al., 1996, 2002). They are found dominantly in the Central Zone or at the eastern margin of the Western Block (Zhao et al., 1999a). In contrast, the MP-granulites, found mostly in the Eastern and Western Blocks, are characterized by pressures below 10 kbar, isobaric cooling following the temperature peak, and possibly anti-clockwise *P–T* paths (Chen and Li, 1996; Liu, 1996; Jin and Li, 1996; Zhao et al., 1999a, 1999b). In the field, these different reaction paths are reflected as plagioclase collars around garnet in decompressed HP rocks and garnet coronas around earlier phases in prograde MP-granulites and have been named ‘white eye-socket’ and ‘red eye-socket’ types, respectively (Ma and Wang, 1994).

An important area for testing the different proposed models for the evolution of the North China Craton is located in northern Shanxi and Hebei Provinces, about 350 km WSW of Beijing, comprising the Hengshan, Wutai and Fuping Complexes (Fig. 1). These all lie within the Central Zone. In the Fuping and Hengshan Complexes, tonalitic–trondhjemitic–granodioritic (TTG) and granitic gneisses dominate, supracrustal assemblages are minor, and mafic rocks identified as strongly deformed gabbroic dykes contain well-preserved granulite-facies assemblages (for recent summary and references, see Kröner et al., 2005a). In contrast, the Wutai Complex situated between these two granulite-bearing units, contains tectonically interdigitated slices of sub-greenschist-facies (structurally uppermost) to amphibolite-facies (structurally lower) volcano-sedimentary rocks and is interpreted as a former arc (Wilde et al., 1997; Zhao et al., 1999c; Wang et al., 2004a). Widely considered as a typical greenstone sequence, attributed to rifting or arc accretion, the Wutai Complex was originally thought to unconformably overlie the Fuping and Hengshan Complexes (Bai, 1986; Ma et al., 1987; Tian et al., 1996). This interpretation, considering the Archaean age of the Wutai Complex rocks (Wilde et al., 1997, 2004; Kröner et al., 2005a), requires the granulites to be older than the Wutai sequence as proposed by several workers (Bai, 1986; Ma et al., 1987; Tian et al., 1996; Zhai et al., 2000; Li et al., 2000a,b; Kusky and Li, 2003). However, the ‘unconformity’ between the Fuping and Wutai Complexes has now been reinterpreted as a detachment structure (Li and Qian, 1991), and SHRIMP dating of zircons from granitoid gneisses of the Fuping Complex revealed that these rocks formed at about the same time as the Hengshan and Wutai Complexes and were overprinted by metamorphism at 1800–1900 Ma (Guan et al., 2002; Zhao et al., 2002a,b). The intention of this study was to establish the age of emplacement and metamorphism of the gabbroic dykes (mafic granulites) in the Hengshan Complex in order to complement the results from the Wutai and Fuping Complexes and thus further test the proposed tectono-metamorphic models for the NCC. Summaries on the composition and evolution of the Hengshan–Wutai–Fuping terrain with contrasting evolutionary models were recently provided by Kusky and Li (2003) and Kröner et al. (2005a).

2. Field relationships in the Hengshan Complex

The gneisses and migmatites of the Hengshan Complex have been described in detail by Li and Qian (1994) and Tian et al. (1996) and are particularly well exposed in three NW–SE trending valleys named Great Wall Valley (Changchenggou), Large Stone Valley (Dashigou) and Small Stone Valley (Xiaoshigou) (Fig. 2). The majority

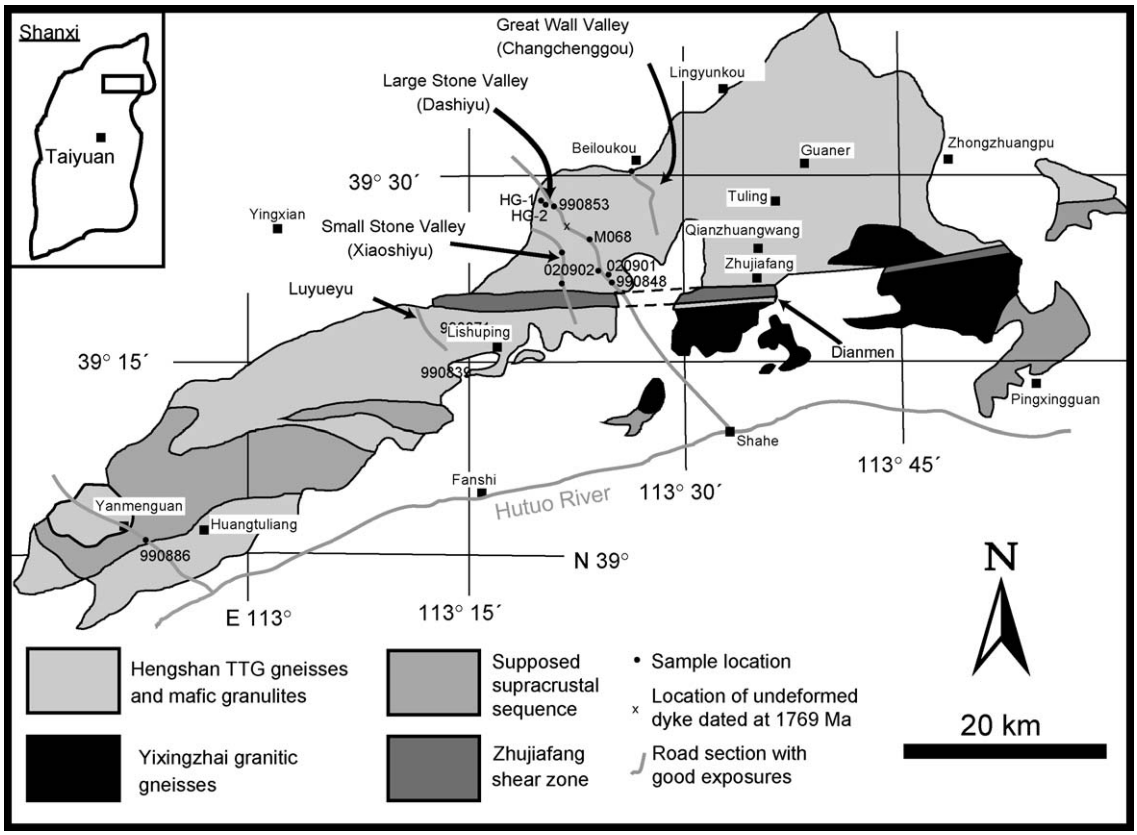

Fig. 2. Overview map of Hengshan terrain showing major rock units, roads, settlements and sample locations mentioned in text. Inset in upper left corner shows Shanxi Province and location of Fig. 2.

of rocks are ductilely deformed, layered orthogneisses of tonalitic, trondhjemitic, granodioritic and granitic composition (TTG-suite) similar to "grey gneisses" in Archaean terrains elsewhere in the world (Li and Qian, 1994; Kröner et al., 2005a,b; Liu et al., 2002, 2004).

The Hengshan rocks are mylonitized in several steeply dipping E–W dextral strike-slip shear zones of which the Zhujiafang shear zone is the most prominent (Fig. 2). In previous studies (e.g. Wang et al., 1991; Li and Qian, 1994) these shear zones were mapped as synclinal infolds of supposed supracrustal rocks of the Wutai Complex. Mylonitization imparted a planar fabric to the sheared rocks in which all evidence of previous deformation is eradicated. This led to an alternation of fine-grained, streaky quartzo-feldspathic gneisses (derived from granitoid gneisses and previously interpreted as clastic metasediments) and amphibolites (deformed gabbroic dykes and previously interpreted as basaltic metavolcanic rocks) in the shear zones where retrogression is common (for details and illustrations, see Kröner et al., 2005b). The Zhujiafang shear zone extends roughly E–W through the centre of the Hengshan (Fig. 2) and has proven to be a boundary with a previously unrecognized regional significance (O'Brien et al., 2005). Structurally, a flat-lying NE–SW to N–S striking foliation in the northern Hengshan is dragged progressively steeper into an E–W orientation as the Zhujiafang shear zone is approached.

Cross-cutting the Hengshan Complex and the Zhujiafang shear zone are numerous steeply dipping NW–SE to NNW–SSE trending unmetamorphosed dolerite dykes. Conventionally analyzed abraded single zircons from one of these dykes yielded an age of 1769.1 ± 2.5 Ma (Halls et al., 2000), thus defining a lower age limit for deformation and metamorphism in the Hengshan Complex. These younger dykes correspond to tholeiitic dyke swarms in the Wutai Mts. dated at 1778 ± 3 Ma (Peng et al., 2005), in the Taihuang Mts. dated at 1781–1765 Ma (Wang et al., 2004b), and in the Taishan Mts. in Shandong Province, dated at 1830 ± 17 Ma (Hou et al., 2006).

Within the gneisses there occur numerous boudins and lensoid layers of dark mafic gneisses or amphibolites of gabbroic composition (Fig. 3), predominantly

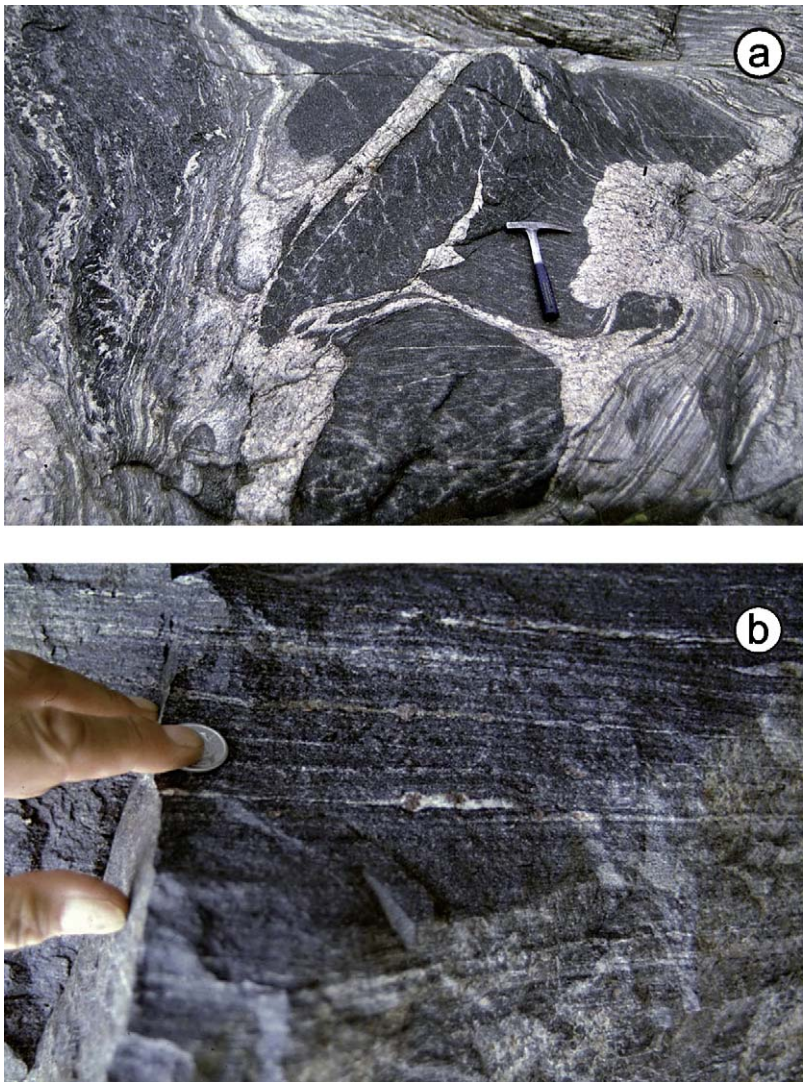

Fig. 3. (a) Fragments of foliated mafic dyke (retrogressed HP mafic granulite) surrounded by unfoliated pegmatoid granite reflecting in situ melting during decompression event and enclosed within ~2.5 Ga grey gneiss. Streambed in upper Large Stone Valley, Hengshan Complex. (b) Foliated mafic granulite with drawn-out plagioclase corona around garnet showing that deformation outlasted high-grade metamorphism. Roadcut in Great Wall Valley, Hengshan Complex.

consisting of an assemblage of hornblende, plagioclase, garnet, clinopyroxene, quartz and rutile which commonly exhibit HP metamorphic assemblages in their cores that are downgraded along the margins (O'Brien et al., 2005). In rare cases, and in particular in low-strain zones such as south of the Zhujiafang shear zone at the southern end of Small Stone Valley, a typical gabbroic primary igneous fabric is preserved (Fig. 4). These amphibolites are remnants of gabbroic dykes that originally intruded into the granitoid rocks as can still be seen at a few localities in low strain zones (Li et al., 2002). Ductile deformation has later rotated these dykes into parallelism with the layering in the enclosing gneisses (cf. Myers, 1978) and, at the same time, caused boudinage (see illustrations in Kröner et al., 2005a,b). The resulting pattern is essentially the same as in high-grade gneiss terrains in SW Greenland and in the Lewisian Complex of Scotland, in the Ancient Gneiss Complex and the Limpopo belt of southern Africa, the Archaean gneisses of the Slave Province of Canada and the Archaean terrain of the northern Yilgarn Craton of Western Australia (see Goodwin, 1991, for further examples). In all these cases the amphibolitic layers and boudins are part of original dyke swarms indicating major extensional events in the history of the complexes in which they occur.

Fig. 4. Crude magmatic layering in gabbroic dyke from which sample Ch 020902 was taken. Dashiyu River, Large Stone Valley, Hengshan Complex.

These mafic dykes, generally known as "high-pressure granulites" in the Chinese literature, have been of particular interest in recent years since they contain metamorphic mineral assemblages recording a HP event with T up to 900 °C and P up to 16 kbar (for summary of data and literature, see Li et al., 1998; Zhai, 1997; Zhao et al., 2001b; O'Brien et al., 2005). Thus, there are two genetically unrelated generations of mafic dykes in the Hengshan Complex. The older shows the HP metamorphic signature and is boudinaged and tectonically rotated into parallelism with the enclosing gneisses, whereas the younger crosscuts all structures and is unmetamorphosed.

3. Summary of petrology and metamorphic evolution of high-pressure granulites

As previously mentioned, within the North China Craton as a whole two fundamentally different types of mafic granulite have been recognized, namely high-pressure and medium-pressure types (e.g. Jin and Li, 1996; Zhao et al., 1999a). The HP-granulites are primarily clinopyroxene-bearing garnet granulites and are known from the Hengshan (Wang et al., 1991; Zhai et al., 1993, 1995; Zhao et al., 2001b), Fuping (Liu, 1996; Zhao et al., 2000a,b) and several other areas (Zhai et al., 1993; Lu and Jin, 1993; Li et al., 1998; Guo et al., 2002). The MP-granulite occurs in the Eastern and Western Blocks (e.g. Liu et al., 1993; Li, 1993) and was interpreted to be a product of magmatic underplating (Zhao et al., 1999b). These two granulite types reflect fundamentally different tectonometamorphic processes and so are generally not found together in a single terrain unless they represent granulite events of different age.

Mafic granulite sheets, boudins and fragments (Fig. 3a) varying from a few tens of cemtimeters to several tens of metres in width are a common feature within the Hengshan grey gneiss complex (Li and Qian, 1994) and their structural relationships have been documented by Kröner et al. (2005a,b). To the north of the Zhujiafang shear zone, relict granulite-facies domains in the mafic boudins are represented by garnet + clinopyroxene-bearing rocks with garnet commonly surrounded by a moat of plagioclase. Locally foliated mafic granulite bodies contain drawn-out plagioclase coronas around garnet showing that deformation outlasted high-grade metamorphism (Fig. 3b).

In contrast, mafic dykes south of the Zhujiafang shear zone locally preserve intrusive features and conspicuous magmatic textures overprinted by delicate garnet coronas rimming plagioclase. In samples preserving the best record of the HP-granulite stage, pale green, lath-like clinopyroxene crystals, several centimeters long, accompanied by millimeter-sized garnets, occur in a fine-grained hornblende–plagioclase matrix. In thin section, the lath-like clinopyroxene occurs in the form of symplectitic intergrowths of diopside and plagioclase and represents the breakdown of a former more jadeite-rich, HP pyroxene. In a second variant of high-pressure granulite, the clinopyroxene contains lamellae and blebs

of plagioclase but without a 'fingerprint-like' symplectite texture. This latter type commonly also contains antiperthite and minor biotite. Details on the metamorphic petrology, mineral chemistry and *P–T* evolution were provided by Zhao et al. (2001b) and O'Brien et al. (2005).

South of the Zhujiafang shear zone, macroscopically visible, magmatic textures are preserved in the central parts of larger (up to 10 m wide) mafic boudins, showing that the protoliths of the mafic boudins were dolerites and gabbros. Within a single mafic body (former dyke or sill), a variety of microtextures can be found ranging from undeformed magmatic texture statically overprinted by granulite-facies or locally just amphibolite-facies, to completely recrystallized amphibolite-facies domains without magmatic relics. The mafic lenses are commonly in sheared contact with their host gneisses, but a critical group of mafic lenses just north of the pass in Yanmenguan valley (Fig. 2) clearly occur as intrusive vertical dykes that cross-cut ductile structures in felsic gneisses and appear to have fine-grained chilled margins (now metamorphosed). Without exception, where this textural variety of metabasite was found in Small Stone Valley and at Dianmen, Luyuegou and Yanmenguan—the location was south of the Zhujiafang shear zone (Fig. 2).

4. Previous geochronology

Two Sm–Nd whole-rock isochron ages have been reported for mafic granulite boudins from the Hengshan with ages of 2851 ± 76 and 2818 ± 86 Ma, respectively, and were interpreted as the magmatic ages of the mafic rocks (Tian et al., 1992). As demonstrated by Kröner et al. (2005b), the majority of gneisses in the Hengshan were emplaced between ~2500 and ~2520 Ma, and the mafic dykes are clearly intrusive into these gneisses. The above Sm–Nd ages are therefore suspect and much too old to represent the crystallization age of the dykes. Chang et al. (1994) have already noted this and pointed out that the individual Sm–Nd analyses come from samples of different dykes and yielded a combined mean eight-point isochron age of 2860 ± 135 Ma with $\varepsilon_{Nd(T)}$ of 6.1, a value which these authors considered too high. They tentatively ascribed the anomalous values to a heterogeneous mantle source but also considered crustal contamination as a potential contributing factor. We suspect that granulite-facies metamorphism caused significant disturbance of the Sm–Nd isotopic system. A similar case has been reported from the nearby high-grade Fuping Complex where a Sm–Nd "isochron age" of 2790 ± 171 Ma, reported from combined amphibolite (mafic dyke), granulite and gneissic samples (Zhang et al., 1991), was shown to be geologically meaningless (Guan et al., 2002).

Kröner et al. (2005a,b) argued that these dykes were emplaced in the late Palaeoproterozoic, followed by high-grade metamorphism at 1850–1880 Ma. This is supported by conventional U–Pb multigrain zircon ages for two samples of mafic granulites with a pooled age of 1850 ± 2 Ma (Chang et al., 1999). The latter authors considered this age to reflect the time of emplacement of the gabbroic dykes but, as demonstrated by O'Brien et al. (2005), most zircons in these rocks are clearly of metamorphic origin and, in our view, date the peak of granulite-facies metamorphism in the Hengshan Complex.

Overgrowth rims on ~2.5 Ga zircons and metamorphic, ball-shaped, grains from TTG-gneisses in the Fuping Complex yielded concordant zircon ages of 1875–1802 Ma and were interpreted to approximate the age of regional high-grade metamorphism (Zhao et al., 2002a). This conclusion is also supported by a ^{40}Ar–^{39}Ar step heating age of 1852 ± 8 Ma for metamorphic garnet from a HP-granulite in the Sanggan area of the NCC, some 100 km NE of the Hengshan Complex (Guo et al., 2001). SHRIMP dating of metamorphic zircons extracted from mafic granulite samples from the same area yielded consistent ages of 1817 ± 12 and 1819 ± 16 Ma and were interpreted to reflect the peak of HP metamorphism (Guo et al., 2005). In summary, the available age data strongly favour HP metamorphism to have occurred in the Palaeoproterozoic.

5. Analytical methods

5.1. SHRIMP II procedure

Zircons were handpicked and mounted in epoxy resin together with chips of the Perth Consortium standard CZ3. The mounts were then polished, cleaned, and photographed in reflected and transmitted light and under cathodoluminescence (CL) to bring out the internal structures (Fig. 5). CL images were obtained on a JEOL JXA-8900RL microprobe at the University of Mainz, and operating conditions were 15 kV accelerating voltage and 12 nA beam current.

Isotopic analyses were performed on the Perth Consortium SHRIMP II and the Beijing SHRIMP II of the Chinese Academy of Geological Sciences whose instrumental characteristics were outlined by de Laeter and Kennedy (1998). The analytical procedures are summarized in Claoué-Long et al. (1995), Nelson (1997) and Williams (1998). The reduced $^{206}Pb/^{238}U$ ratios

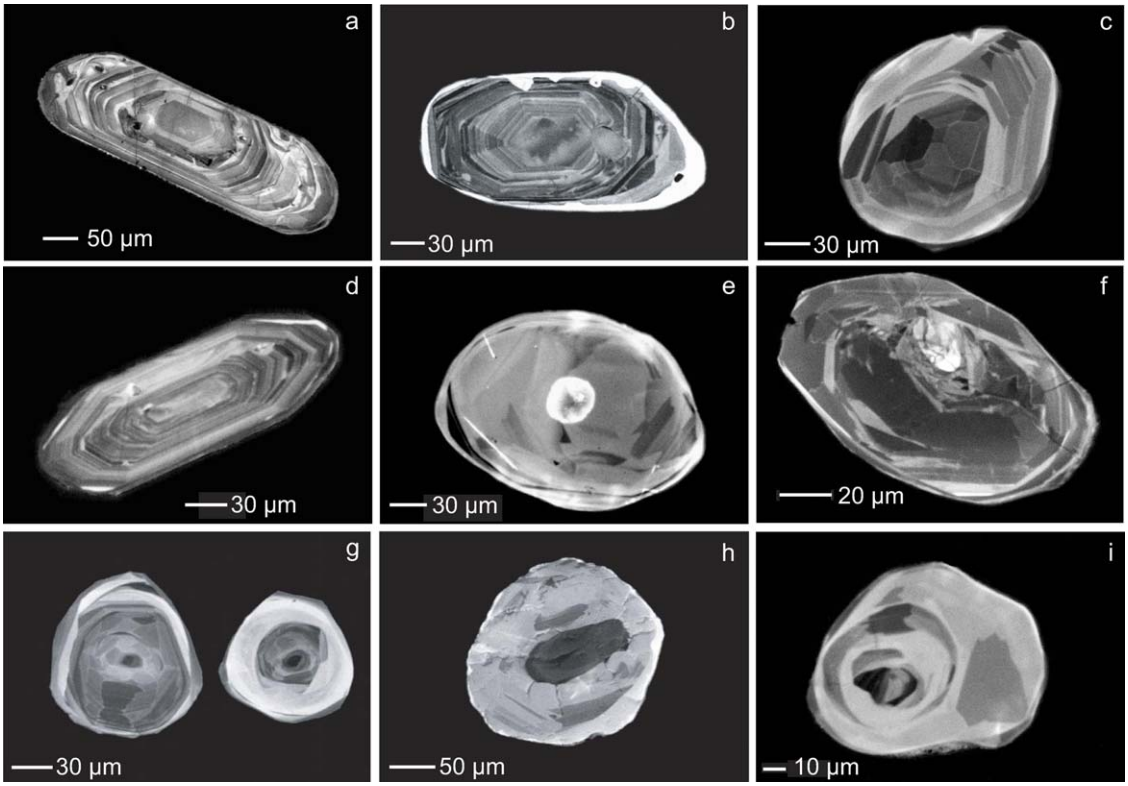

Fig. 5. Cathodoluminescence images of selected magmatic and metamorphic zircons from HP mafic granulites (gabbroic dykes), Hengshan Complex, North China Craton. (a) Rounded magmatic grain from sample Ch 020901, showing oscillatory zoning. (b) Magmatic grain from same sample with thin metamorphic overgrowth. (c) Metamorphic grain from same sample showing ball-shaped nature and well-developed sector zoning. (d) Rounded magmatic grain from sample Ch 020902 with fine oscillatory zoning. (e) Metamorphic grain from sample MO68 with burn mark of ion beam in the centre. (f) Metamorphic grain with fine sector zoning from sample HG-2. (g) Two sector-zoned metamorphic zircons from sample Ch 990853. (h) Sector-zoned, low-U metamorphic grain with dark, high-U core from sample Ch 980871. (i) Broad sector zoning in metamorphic zircon from sample Ch 990886.

for CZ3 were normalized to 0.09143, which is equivalent to an age of 564 Ma. The uncertainty in the ratio $^{206}Pb^{*}/U$ of all standard zircons during this study was between 1.33 and 1.65% for the Perth instrument and 0.79% for the Beijing instrument. Analyses of samples and standards were alternated to allow assessment of Pb^{+}/U^{+} discrimination. Sensitivity varied between 18 and 24 cps/ppm/nA Pb on the Beijing instrument and 20 and 22 on the Perth instrument. Raw data reduction followed the method described by Nelson (1997). Common Pb is considered to be mainly surface-related (Kinny, 1986), and corrections have been applied using the ^{204}Pb-correction method and assuming the isotopic composition of Broken Hill (Cumming and Richards, 1975). The analytical data are presented in Tables 2 and 3. Errors given on individual analyses are based on counting statistics and are at the 1-sigma level and include the uncertainty of the standard added in quadrature. Stern (1997) provided a detailed account of the counting error assessment for SHRIMP analyses. Errors for pooled analyses are reported at the 2-sigma level. The ages and 2σ errors of intercepts of the best-fit line with Concordia were calculated using the ISOPLOT 3-Excel-spreadsheet program of Ludwig (2003). These errors were not multiplied with the square root of the MSWD since the absolute value of the intercept error is strongly model-dependent.

5.2. Single zircon evaporation

Our laboratory procedures as well as comparisons with conventional and ion-microprobe zircon dating are detailed in Kröner et al. (1991) and Kröner and Hegner (1998). Isotopic measurements were carried out on a Finnigan-MAT 261 mass spectrometer at the Max-Planck-Institut für Chemie in Mainz.

The calculated ages and uncertainties are based on the means of all ratios evaluated and their 2σ mean

errors. Mean ages and errors for several zircons from the same sample are presented as weighted means of the entire population. During the course of this study we repeatedly analyzed fragments of large, homogeneous zircon grains from the Palaborwa Carbonatite, South Africa. Conventional U–Pb analyses of six separate grain fragments from this sample yielded a $^{207}Pb/^{206}Pb$ age of 2052.2 ± 0.8 Ma (2σ, W. Todt, unpublished data), whereas the mean $^{207}Pb/^{206}Pb$ ratio for 21 grains, evaporated individually over a period of 12 months, is 0.126634 ± 0.000026 (0.2%, 2σ error of the population), corresponding to an age of 2051.8 ± 0.4 Ma, identical to the conventional Pb–Pb age. The above error is considered the best estimate for the reproducibility of our evaporation data and corresponds approximately to the (mean) error reported for individual analyses in this study (Table 3). In the case of combined data sets the $2\sigma_m$ error may become very low, and whenever this error was less than the reproducibility of the internal standard, we have used the latter value (that is, an assumed 2σ error of 0.2%).

The analytical data are presented in Table 3, and the $^{207}Pb/^{206}Pb$ spectra are shown in histograms that permit visual assessment of the data distribution from which the ages are derived. The evaporation technique provides only Pb isotopic ratios, and there is no a priori way to determine whether a measured $^{207}Pb/^{206}Pb$ ratio reflects a concordant age. Thus, all $^{207}Pb/^{206}Pb$ ages determined by this method are necessarily *minimum* ages. However, many studies have demonstrated that there is a very strong likelihood that these data represent true zircon crystallization ages when (1) the $^{207}Pb/^{206}Pb$ ratio does not change with increasing temperature of evaporation and/or (2) repeated analyses of grains from the same sample at high evaporation temperatures yield the same isotopic ratios within error. Comparative studies by evaporation, conventional U–Pb dating, and ion-microprobe analysis have shown this to be correct (Kröner et al., 1991, 1999; Cocherie et al., 1992; Jaeckel et al., 1997; Karabinos, 1997).

6. Formation of metamorphic zircon at high temperature and high pressure

The closure temperature of zircon for the U–Pb system is well above 900 °C (Mezger and Krogstad, 1997; Möller et al., 2002), and the experimental determination of diffusion parameters for U, Th, Pb and Hf in zircon (e.g. Cherniak et al., 1997; Lee et al., 1997) also support this view. This makes it almost certain that metamorphic zircon records the isotopic composition near or at its growth stage. Inclusion–host relationships such as phengite in zircon (Kröner and Willner, 1998) or isotopically almost undisturbed zircon in diamond from ultra-high pressure metamorphic rocks (Claoué-Long et al., 1991) can be used to constrain the age of zircon growth to parts of the metamorphic history. Ovoid to spherical, multifaceted zircons that grew during peak metamorphic conditions (Hoskin and Black, 2000; Pidgeon et al., 2000; Corfu et al., 2003) are known from ultra-high pressure rocks in the Kokchetav massif, Kazakhstan (Claoué-Long et al., 1991; Sobolev et al., 1992) and the Dora Maira Massif, Western Alps (Gebauer et al., 1993; Schertl and Schreyer, 1995). In these rocks, phases that were stable near maximum pressure conditions, such as diamond, Si-rich phengite, jadeite-rich clinopyroxene, kyanite, pyrope, talc, coesite or rutile were found enclosed within the zircons. Such football-shaped zircons also occur in rocks of many granulite terrains such as the Saxonian granulite massif, Germany (Kröner et al., 1998), the Bohemian Massif, Czech Republic (Kröner et al., 2000), the Limpopo belt, South Africa (Jaeckel et al., 1997), and Enderby Land, Antarctica (Kelly and Harley, 2005). Concordant U–Pb SHRIMP ages for such zircons were therefore interpreted as dating the peak of metamorphism. Furthermore, closure of zircon to Pb diffusion in these rocks probably occurred at about the same time as closure of garnet and clinopyroxene to Nd diffusion (Mezger and Krogstad, 1997). These two factors, together with resistance to resetting and protection of inclusions, make metamorphic zircon probably the best currently available mineral to allow precise dating of regional high-grade metamorphism (Krogh, 1993; Kröner et al., 1994; Mezger and Krogstad, 1997; Pidgeon et al., 2000; Möller et al., 2002).

Following zircon formation, the diffusive modification of zircon isotopic patterns under known crustal metamorphic conditions and timescales is unlikely (Cherniak et al., 1997; Lee et al., 1997), but the causes and timing of possible zircon dissolution, recrystallization or new growth must still be evaluated.

7. Sample location and zircon geochronology

We have dated igneous and metamorphic zircons from several HP-granulite samples collected from boudinaged mafic dykes in the Hengshan Complex, and the locations are shown in Fig. 2. Sample Ch 020901 is from the core of a HP-granulite boudin exposed in a streambed behind a small restaurant in Large Stone Valley along the asphalt road from Shahe to the NW (longitude 113°23′49.9″E; latitude 39°27′00.1″N). The petrography and mineral chemistry of this rock was described by O'Brien et al. (2005). Sample Ch 020902 represents a gabbroic

Fig. 6. Field photograph of pegmatoid melt patches resulting from isothermal decompression in large HP metagabbro boudin (sample Ch 990839), Small Stone Valley, Hengshan Complex.

dyke, some 12–15 m wide and exposed in the bed of the Dashiyu River in Large Stone Valley, about 400 m WNW of sample Ch 020901 (longitude 113°23′53.6″E; latitude 39°27′06.9″N). The dyke shows well-preserved relict magmatic layering (Fig. 4).

Sample MO68 represents a HP-granulite boudin (retrograded eclogite) surrounded by layered tonalitic gneiss and collected from a roadcut between Yangqian and Zhaojiayao villages along the Yingxian-Shahe asphalt road in Large Stone Valley (Fig. 2, longitude 113°22′20.6″E; latitude 39°27′28.9″N). Another HP-granulite is represented by sample HG-2, collected from a mafic dyke boudin within migmatitic gneisses in the gorge of the Dashiyu River in Large Stone Valley (longitude 113°19′59.1″E; latitude 39°28′46.6″N). Possibly because of infiltration of fluids from the hosting migmatitic gneisses, nearly all pyroxene and garnet in this sample have been retrograded into hornblende, biotite and epidote. Sample Ch 990853 is from a near-horizontal mafic dyke with an eclogitic mineral assemblage and collected from a fresh roadcut in the western half of the asphalt road pass in Large Stone Valley NW of Shahe town (Fig. 2, longitude 113°26′56.5″E; latitude 39°30′11.7″N). Sample Ch 980871 represents another mafic dyke with eclogitic mineralogy and was collected in a fresh road cut in Small Stone Valley (longitude 113°27′38.4″E; latitude 39°28′01.9″N). Sample 990886 represents a medium-pressure mafic granulite collected from a roadcut SW of the Wildgoose-gate pass (Yanmenguan) in the SW of the Hengshan Complex (longitude 112°52′04″E; latitude 39°08′52″N).

Sample Ch 990839 represents a spectacular example of a large gabbroic boudin in Small Stone Valley (113°27′59.5″E, 39°27′50.7″N) containing coarse-grained pegmatoid melt patches (Fig. 6) that probably formed during isothermal decompression shortly after the peak of HP-metamorphism. The sample represents about 4 kg of 3–6 cm fragments of the pegmatoid melt phase. Lastly, granite gneiss sample HG-1 was collected in the deep gorge of the Dashiyu River in Large Stone Valley, within a few metres to sample HG-2 (see coordinates above).

7.1. Magmatic emplacement and xenocryst ages

Igneous zircons are rare in these dykes and were only found at two localities in Large Stone Valley (Dashigou). The zircons of sample Ch 020901 comprise two morphological types with one consisting of long-prismatic grains, well rounded at their terminations, as is typical of zircons subjected to high-grade metamorphism (Silver, 1969; Vavra, 1990; Kröner et al., 1994; Hoskin and Black, 2000), and oscillatory zoning revealing a magmatic origin (Fig. 6). Some of these grains have high-luminescent (low-U), structureless, narrow rims (Fig. 6), too thin to be measured on SHRIMP and presumably reflecting metamorphic overgrowth. These are similar to magmatic zircons in TTG-gneisses previously described from the Hengshan and Fuping Complexes (Kröner et al., 2005b; Zhao et al., 2002a). The other type consists of rare oval to spherical, multifaceted grains with well-developed sector zoning (Fig. 6) and this is of metamorphic origin.

Table 1
Analytical data for zircons from gabbroic dyke (HP-granulite) samples Ch 020901, Ch 020902, M068 and pegmatoid melt patch sample Ch 990839, Hengshan Complex[a]

Sample no.	U (ppm)	Th (ppm)	$^{206}Pb/^{204}Pb$	$^{208}Pb/^{206}Pb$	$^{207}Pb/^{206}Pb$	$^{206}Pb/^{238}U$	$^{207}Pb/^{235}U$	$^{206}Pb/^{238}U$ age ± 1σ	$^{207}Pb/^{235}U$ age ± 1σ	$^{207}Pb/^{206}Pb$ age ± 1σ
Ch 901-1.1[b]	89	12	9888	0.0468 ± 63	0.1165 ± 32	0.3483 ± 50	5.592 ± 182	1926 ± 24	1915 ± 28	1902 ± 49
Ch 901-1.2	147	7	11929	0.0230 ± 34	0.1159 ± 19	0.3561 ± 46	5.691 ± 127	1964 ± 22	1930 ± 22	1894 ± 30
Ch 901-2-1	111	3	8446	0.0220 ± 43	0.1180 ± 24	0.3479 ± 48	5.660 ± 147	1925 ± 23	1925 ± 22	1926 ± 36
Ch 901-3.1	1068	909	1116	0.1889 ± 22	0.1299 ± 10	0.3056 ± 32	5.473 ± 77	1719 ± 16	1896 ± 12	2097 ± 14
Ch 901-4-1	84	4	9656	0.0287 ± 45	0.1182 ± 26	0.3551 ± 50	5.786 ± 159	1959 ± 24	1944 ± 23	1929 ± 39
Ch 901-5.1	94	3	10402	0.0120 ± 68	0.1178 ± 34	0.3521 ± 48	5.719 ± 191	1945 ± 23	1934 ± 28	1923 ± 52
Ch 901-6-1	96	4	113869	0.0182 ± 14	0.1176 ± 16	0.3527 ± 47	5.718 ± 115	1948 ± 22	1934 ± 17	1920 ± 24
Ch 901-7.1	95	8	100000	0.0307 ± 13	0.1173 ± 17	0.2991 ± 51	4.837 ± 114	1687 ± 25	1791 ± 20	1915 ± 25
Ch 901-8.1	116	2.6	25100	0.0082 ± 15	0.1174 ± 14	0.3246 ± 56	5.254 ± 116	1812 ± 27	1861 ± 19	1917 ± 22
Ch 901-9.1	82	3.4	8762	0.0169 ± 23	0.1170 ± 18	0.3127 ± 55	5.046 ± 124	1754 ± 27	1827 ± 21	1911 ± 27
Ch 901-10.1	88	2.1	9594	0.0096 ± 29	0.1172 ± 19	0.3189 ± 55	5.156 ± 130	1785 ± 27	1845 ± 21	1914 ± 29
Ch 901-11.1	102	4.7	3893	0.0125 ± 50	0.1173 ± 27	0.3245 ± 59	5.246 ± 163	1812 ± 29	1860 ± 26	1915 ± 41
Ch 901-12.1	117	2.7	13085	0.0159 ± 21	0.1171 ± 17	0.2855 ± 47	4.609 ± 109	1619 ± 24	1751 ± 19	1912 ± 26
Ch 901-13.1	96	3.7	5534	0.0214 ± 34	0.1170 ± 20	0.3121 ± 55	5.035 ± 133	1751 ± 27	1825 ± 22	1911 ± 31
Ch 901-14.1	121	5.7	17068	0.0196 ± 18	0.1172 ± 16	0.3137 ± 55	5.072 ± 120	1759 ± 27	1831 ± 20	1915 ± 25
Ch 901-14.2	88	1.4	11728	0.0351 ± 27	0.1265 ± 21	0.3492 ± 65	6.092 ± 161	1931 ± 31	1989 ± 23	2050 ± 29
Ch 901-15.1	78	5.9	100000	0.0382 ± 16	0.1175 ± 19	0.3441 ± 64	5.573 ± 145	1906 ± 31	1912 ± 22	1918 ± 29
Ch 901-16.1	109	3.7	100000	0.0146 ± 8	0.1365 ± 17	0.4002 ± 72	7.530 ± 174	2170 ± 33	2177 ± 21	2183 ± 22
Ch 901-17.1	103	4.7	100000	0.0170 ± 9	0.1173 ± 16	0.3444 ± 61	5.571 ± 133	1908 ± 25	1912 ± 20	1916 ± 25
Ch 902-1.1	69	0.6	1889	0.0119 ± 49	0.1173 ± 25	0.3299 ± 40	5.334 ± 139	1838 ± 19	1874 ± 22	1915 ± 38
Ch 902-2.1	63	0.5	24763	0.0064 ± 13	0.1171 ± 15	0.3191 ± 39	5.149 ± 97	1785 ± 19	1844 ± 16	1912 ± 23
Ch 902-3.1	62	1.5	4891	0.0145 ± 25	0.1172 ± 19	0.2674 ± 30	4.322 ± 89	1528 ± 15	1698 ± 17	1914 ± 28
Ch 902-4.1	66	0.6	37900	0.0097 ± 10	0.1174 ± 18	0.3169 ± 37	5.128 ± 104	1774 ± 18	1841 ± 17	1916 ± 27
Ch 902-5.1	77	0.7	14018	0.0033 ± 15	0.1174 ± 18	0.3104 ± 33	5.025 ± 98	1743 ± 16	1824 ± 16	1917 ± 27
Ch 901-6.1	374	227	9093	0.1656 ± 13	0.1613 ± 8	0.3894 ± 34	8.658 ± 91	2120 ± 16	2303 ± 10	2469 ± 8
Ch 902-7.1	54	0.8	4153	0.0069 ± 31	0.1171 ± 22	0.2996 ± 36	4.838 ± 114	1689 ± 18	1792 ± 20	1913 ± 33
Ch 902-8.1	69	0.6	3151	0.0008 ± 33	0.1171 ± 21	0.3424 ± 43	5.529 ± 127	1898 ± 21	1905 ± 20	1913 ± 32
M062-1.1	104	1.7	8210	0.0148 ± 27	0.1135 ± 22	0.3153 ± 44	4.935 ± 124	1767 ± 21	1808 ± 21	1856 ± 35
M062-2.1	56	0.5	3492	0.0179 ± 62	0.1133 ± 39	0.3139 ± 52	4.903 ± 198	1760 ± 26	1803 ± 33	1853 ± 61
M062-3-1	112	1.5	223065	0.0123 ± 8	0.1128 ± 17	0.3071 ± 38	4.777 ± 97	1726 ± 19	1781 ± 17	1845 ± 26
M062-4.1	87	0.9	8875	0.0100 ± 24	0.1139 ± 21	0.3087 ± 41	4.851 ± 116	1734 ± 20	1794 ± 20	1863 ± 33
M062-5.1	89	2.1	7074	0.0099 ± 30	0.1135 ± 22	0.3232 ± 43	5.058 ± 124	1805 ± 21	1829 ± 21	1856 ± 34
Ch839-1.1	1447	61	3388	0.0177 ± 5	0.1135 ± 3	0.3683 ± 10	5.761 ± 152	2021 ± 45	1941 ± 23	1855 ± 5
Ch839-2.1	354	8.4	1093	0.0111 ± 19	0.1127 ± 10	0.3125 ± 82	4.856 ± 138	1753 ± 40	1795 ± 24	1843 ± 15
Ch839-3.1	69	1.9	6294	0.0099 ± 20	0.1135 ± 13	0.3269 ± 87	5.114 ± 155	1823 ± 42	1838 ± 25	1856 ± 21
Ch839-4.1	88.5	1.4	4701	0.0019 ± 25	0.1129 ± 14	0.3227 ± 85	5.022 ± 153	1803 ± 41	1823 ± 25	1846 ± 22
Ch839-5.1	1905	103	833	0.0206 ± 11	0.1126 ± 5	0.2489 ± 65	3.865 ± 104	1433 ± 33	1606 ± 22	1842 ± 9
Ch839-6.1	2966	94	895	0.0104 ± 8	0.1126 ± 4	0.2887 ± 75	4.477 ± 119	1635 ± 37	1727 ± 22	1840 ± 6
Ch839-7.1	797	28	636	0.0153 ± 15	0.1138 ± 7	0.3524 ± 92	5.529 ± 151	1946 ± 44	1905 ± 23	1861 ± 11
Ch839-8.1	93	2.4	8885	0.0083 ± 19	0.1130 ± 12	0.3337 ± 88	5.201 ± 154	1856 ± 42	1853 ± 25	1849 ± 19
Ch839-9.1	5110	113	1537	0.0122 ± 5	0.1128 ± 3	0.2670 ± 69	4.154 ± 110	1526 ± 35	1665 ± 21	1845 ± 4

[a] Zircons from sample Ch 990839 were analyzed on SHRIMP II in Perth, all other samples on SHRIMP II in Beijijng.
[b] 1-1 is spot 1 on grain 1, 1-2 is spot 2 on grain 1, etc.

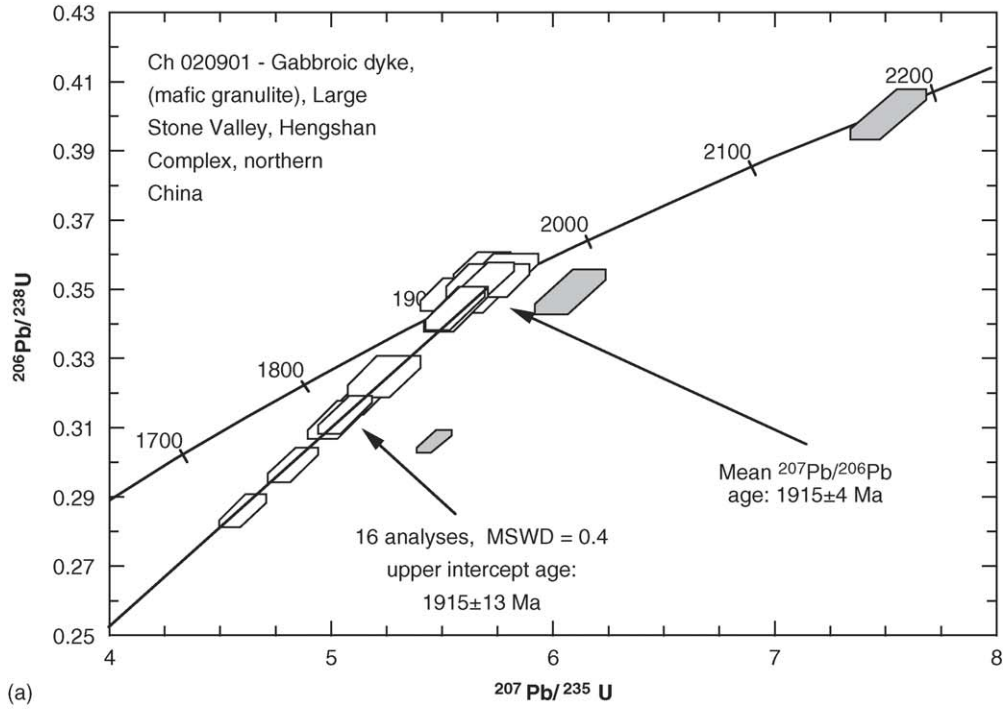

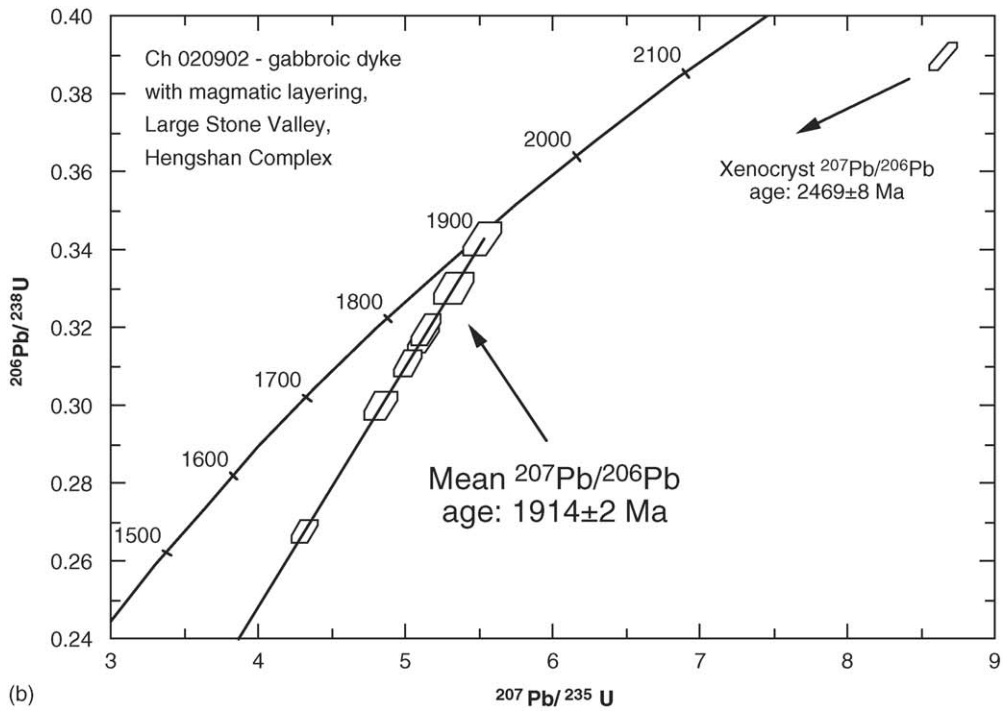

Fig. 7. Concordia diagrams showing SHRIMP II data for spot analyses from magmatic zircon grains of gabbroic dyke samples in the Hengshan Complex (for locations see Fig. 2). (a) Sample Ch 020901, Large Stone Valley. Data boxes are defined by standard errors in $^{207}Pb/^{235}U$ and $^{206}Pb/^{238}U$. (b) Sample Ch 020902, Dashiyu River, Large Stone Valley. Errors as in (a).

Table 2
Analytical data (Perth SHRIMP II) for zircons of gabbroic dyke sample HG-2 and late granite gneiss sample HG-1, Hengshan Complex

Sample and spot no.	U (ppm)	Th (ppm)	$^{206}Pb/^{204}Pb$	$^{208}Pb/^{206}Pb$	$^{207}Pb/^{206}Pb$	$^{206}Pb/^{238}U$	$^{207}Pb/^{235}U$	$^{206}Pb/^{238}U$ age $\pm 1\sigma$	$^{207}Pb/^{235}U$ age $\pm 1\sigma$	207/206 age $\pm 1\sigma$
HG-1										
HG1-1	11109	17	1163	0.0447 ± 32	0.0830 ± 14	0.0824 ± 7	0.94 ± 2	511 ± 4	675 ± 10	1270 ± 34
HG1-2	483	5	5000	0.0127 ± 14	0.1101 ± 8	0.2553 ± 23	3.88 ± 5	1466 ± 12	1609 ± 10	1801 ± 13
HG1-3	595	7	4545	0.0123 ± 10	0.1124 ± 6	0.2971 ± 27	4.60 ± 5	1677 ± 13	1750 ± 9	1839 ± 10
HG1-4	747	9	1000	0.0658 ± 39	0.0983 ± 18	0.0963 ± 9	1.30 ± 3	593 ± 5	848 ± 12	1591 ± 34
HG1-5	110	21	3333	0.0615 ± 30	0.1481 ± 16	0.4090 ± 47	8.35 ± 14	2210 ± 21	2270 ± 15	2323 ± 18
HG1-6	827	17	5556	0.0065 ± 11	0.1019 ± 6	0.1873 ± 16	2.63 ± 3	1107 ± 9	1309 ± 8	1658 ± 11
HG1-7	880	7	826	0.1061 ± 50	0.0905 ± 22	0.0592 ± 5	0.74 ± 2	371 ± 3	562 ± 12	1436 ± 46
HG1-8	411	130	2857	0.0232 ± 19	0.1122 ± 10	0.3206 ± 30	4.96 ± 7	1793 ± 14	1813 ± 11	1836 ± 15
HG1-9	1189	10	1724	0.0789 ± 32	0.0909 ± 15	0.0602 ± 5	0.76 ± 1	377 ± 3	571 ± 9	1445 ± 31
HG1-10	848	12	1587	0.0878 ± 35	0.0963 ± 16	0.0742 ± 7	0.98 ± 2	461 ± 4	696 ± 10	1553 ± 32
HG1-11	1506	15	2326	0.0268 ± 15	0.0781 ± 7	0.0979 ± 8	1.05 ± 1	602 ± 5	731 ± 7	1149 ± 19
HG1-12	905	5	2228	0.0522 ± 27	0.1019 ± 13	0.1153 ± 10	1.62 ± 3	703 ± 6	978 ± 10	1660 ± 24
HG1-13	930	11	2273	0.0292 ± 19	0.1006 ± 10	0.1346 ± 12	1.87 ± 3	814 ± 7	1069 ± 9	1635 ± 18
HG1-14	336	3	2174	0.0033 ± 21	0.1132 ± 11	0.3235 ± 31	5.05 ± 7	1807 ± 15	1827 ± 12	1851 ± 18
HG1-15	1485	11	1429	0.0033 ± 11	0.1151 ± 6	0.3217 ± 27	5.11 ± 5	1798 ± 13	1837 ± 9	1882 ± 9
HG1-16	339	3	4662	0.0062 ± 15	0.1128 ± 8	0.3216 ± 30	5..00 ± 6	1797 ± 14	1819 ± 11	1845 ± 14
HG1-17	1118	7	5882	0.0002 ± 7	0.1156 ± 4	0.3207 ± 27	5.11 ± 5	1793 ± 13	1838 ± 8	1889 ± 7
HG1-18	62	55	2128	0.2448 ± 51	0.1667 ± 23	0.4730 ± 68	10.87 ± 23	2497 ± 30	2512 ± 20	2525 ± 24
HG1-19	1744	15	20000	0.0034 ± 3	0.1143 ± 3	0.3212 ± 26	5.06 ± 5	1796 ± 13	1829 ± 8	1868 ± 5
HG1-20	114	3	2326	0.0051 ± 40	0.1136 ± 20	0.3306 ± 40	5.18 ± 12	1841 ± 19	1849 ± 19	1858 ± 32
HG1-21	899	17	2174	0.0309 ± 17	0.1048 ± 8	0.2164 ± 19	3.13 ± 4	1263 ± 10	1439 ± 10	1710 ± 15
HG1-22	1246	7	2273	0.0178 ± 14	0.1067 ± 7	0.2335 ± 20	3.44 ± 4	1353 ± 10	1513 ± 9	1744 ± 12

Table 2 (*Continued*)

Sample and spot no.	U (ppm)	Th (ppm)	$^{206}Pb/^{204}Pb$	$^{208}Pb/^{206}Pb$	$^{207}Pb/^{206}Pb$	$^{206}Pb/^{238}U$	$^{207}Pb/^{235}U$	$^{206}Pb/^{238}U$ age ± 1σ	$^{207}Pb/^{235}U$ age ± 1σ	207/206 age ± 1σ
HG-2										
HG2-1	12	2	3846	0.0449 ± 94	0.1148 ± 44	0.3225 ± 52	5.11 ± 22	1802 ± 25	1837 ± 37	1877 ± 69
HG2-2	90	1	10000	0.0026 ± 17	0.1110 ± 10	0.3315 ± 32	5.07 ± 7	1845 ± 16	1831 ± 12	1815 ± 16
HG2-3	275	12	11111	0.0144 ± 9	0.1116 ± 6	0.3116 ± 27	4.79 ± 5	1748 ± 13	1784 ± 9	1826 ± 9
HG2-4	255	5	20000	0.0051 ± 7	0.1118 ± 5	0.3265 ± 29	5.04 ± 5	1822 ± 14	1825 ± 9	1830 ± 8
HG2-5	356	12	20000	0.0101 ± 5	0.1115 ± 4	0.2942 ± 25	4.52 ± 4	1662 ± 13	1735 ± 8	1823 ± 6
HG2-6	20	4	2778	0.0601 ± 82	0.1148 ± 38	0.3106 ± 42	4.92 ± 18	1744 ± 21	1805 ± 32	1877 ± 60
HG2-7	199	5	25000	0.0064 ± 8	0.1121 ± 6	0.3238 ± 30	5.00 ± 6	1808 ± 15	1820 ± 10	1833 ± 10
HG2-8	344	129	20000	0.1060 ± 9	0.1094 ± 5	0.3181 ± 29	4.80 ± 5	1780 ± 14	1784 ± 9	1789 ± 9
HG2-9	509	196	6250	0.1128 ± 13	0.1096 ± 7	0.2128 ± 19	3.21 ± 4	1244 ± 10	1461 ± 9	1792 ± 11
HG2-10	690	85	16667	0.0366 ± 7	0.1102 ± 4	0.3116 ± 27	4.73 ± 5	1749 ± 13	1773 ± 8	1803 ± 7
HG2-11	283	8	14286	0.0068 ± 8	0.1123 ± 6	0.3315 ± 30	5.13 ± 6	1846 ± 14	1842 ± 9	1837 ± 9
HG2-12	283	8	33333	0.0087 ± 7	0.1137 ± 5	0.3341 ± 30	5.23 ± 6	1858 ± 15	1858 ± 9	1859 ± 8
HG2-13	1446	14	5000	0.0088 ± 9	0.0967 ± 5	0.1382 ± 12	1.84 ± 2	835 ± 7	1061 ± 7	1561 ± 10
HG2-14	10	<1	9091	0.0335 ± 162	0.1238 ± 75	0.3423 ± 72	5.84 ± 39	1898 ± 35	1952 ± 58	2011 ± 108
HG2-15	28	3	3704	0.0278 ± 59	0.1113 ± 29	0.3288 ± 46	5.04 ± 16	1833 ± 23	1827 ± 27	1820 ± 48
HG2-16	282	8	25000	0.0076 ± 6	0.1119 ± 6	0.3268 ± 29	5.04 ± 5	1823 ± 14	1826 ± 9	1830 ± 9
HG2-17	331	11	16666	0.0077 ± 7	0.1122 ± 5	0.3254 ± 29	5.03 ± 5	1816 ± 14	1825 ± 9	1835 ± 9
HG2-18	278	7	33333	0.0075 ± 6	0.1130 ± 5	0.3319 ± 30	5.17 ± 6	1847 ± 14	1848 ± 9	1848 ± n9
HG2-19	600	280	4000	0.1450 ± 18	0.1008 ± 9	0.1182 ± 11	1.64 ± 2	720 ± 6	987 ± 8	1640 ± 16
HG2-20	242	6	7692	0.0084 ± 13	0.1122 ± 8	0.3241 ± 30	5.02 ± 6	1810 ± 14	1822 ± 10	1836 ± 12
HG2-21	82	7	2778	0.0318 ± 34	0.1155 ± 17	0.3287 ± 36	5.23 ± 10	1832 ± 17	1858 ± 16	1887 ± 26
HG2-22	386	166	33333	0.1270 ± 9	0.1104 ± 5	0.2758 ± 24	4.20 ± 4	1570 ± 12	1674 ± 9	1806 ± 8
HG2-23	269	8	20000	0.0081 ± 6	0.1121 ± 5	0.3292 ± 30	5.09 ± 5	1834 ± 14	1834 ± 9	1834 ± 8
HG2-24	464	206	10000	0.1295 ± 10	0.1091 ± 5	0.2357 ± 21	3.54 ± 4	1364 ± 11	1537 ± 8	1784 ± 8
HG2-25	238	70	4762	0.0791 ± 20	0.1123 ± 10	0.2311 ± 22	3.58 ± 5	1340 ± 11	1545 ± 11	1837 ± 16
HG2-26	560	179	8333	0.0986 ± 13	0.1060 ± 6	0.1593 ± 14	2.33 ± 3	953 ± 8	1221 ± 8	1732 ± 11
HG2-27	203	83	20000	0.1178 ± 13	0.1120 ± 7	0.3200 ± 30	4.94 ± 6	1790 ± 15	1809 ± 10	1832 ± 11
HG2-28	373	10	25000	0.0077 ± 6	0.1124 ± 5	0.3235 ± 29	5.01 ± 5	1807 ± 14	1821 ± 9	1838 ± 8

A total of 17 magmatic grains was analyzed on the Beijing SHRIMP, and the results are listed in Table 1 and in the concordia diagram of Fig. 7a. A group of eight grains is concordant with a weighted mean $^{207}Pb/^{206}Pb$ age of 1915 ± 4 Ma, whereas six grains are variably discordant reflecting recent Pb-loss and showing an alignment suggesting that they belong to the same age group as the concordant grains. The discordant analyses probably reflect (hydrothermal?) alteration of variably metamict portions of the igneous grains (Geisler et al., 2003). We exclude instrumentally biased discordancy due to wrong U–Pb calibration in which case reverse

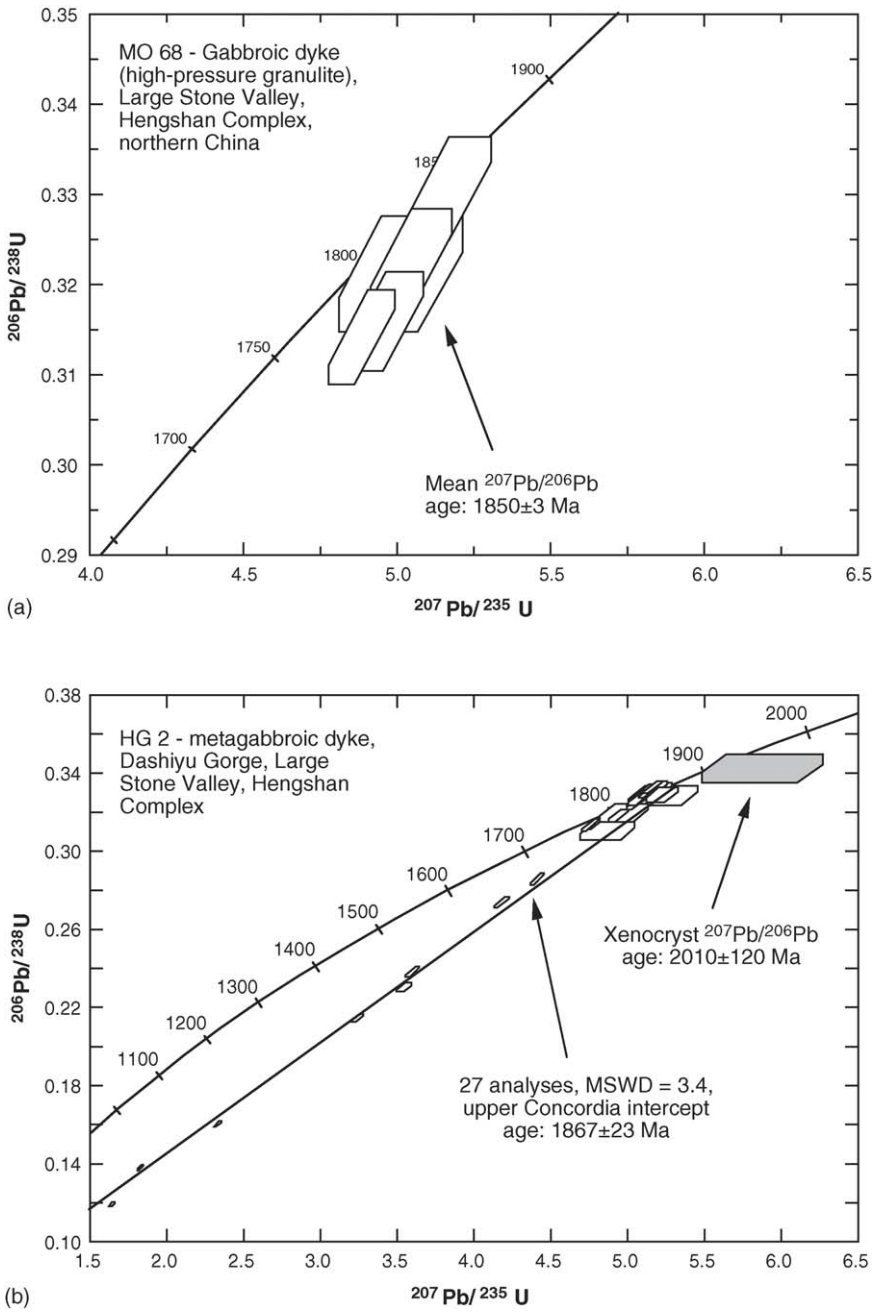

Fig. 8. Concordia diagrams showing SHRIMP II data for spot analyses from metamorphic zircon grains from gabbroic dyke samples (HP mafic granulites) in the Hengshan Complex (for locations see Fig. 2, uncertainties as in Fig. 7a). (a) Sample MO68, roadcut in Large Stone Valley, Hengshan Complex. (b) Sample HG-2, gorge of Dashiyu River, lower Large Stone Valley.

discordancy should also be observed. Recent Pb-loss was also found in zircons from the surrounding TTG-gneisses (Kröner et al., 2005b).

A best-fit line through all data points (MSWD = 0.14) produces a concordia intercept age of 1915 ± 13 Ma (Fig. 7a). Three additional grains, one concordant and two discordant, are significantly older with $^{207}Pb/^{206}Pb$ ages of 2050 ± 29, 2097 ± 14 and 2183 ± 22 Ma (Table 1; Fig. 7). We interpret the age of 1915 Ma as reflecting the time of emplacement of the gabbroic dyke, whereas the older ages are from xenocrystic zircons which were incorporated into the gabbroic melt during magma formation or ascent and thus reflect crustal contamination. Zircon ages around 2100 Ma were reported from the Hengshan gneisses by Kröner et al. (2005b).

The zircons in sample Ch 020902 are exclusively of the long-prismatic type with rounded terminations, simple internal growth structures and only rare oscillatory, magmatic zoning (Fig. 6). Eight grains were analyzed on the Beijing SHRIMP and these have experienced variable degrees of recent Pb-loss (Table 1; Fig. 7b). Seven analyses, with one virtually concordant, are well aligned and define a mean $^{207}Pb/^{206}Pb$ age of 1914 ± 2 Ma. The data can be fitted to a discordia line (MSWD = 0.01) with an upper concordia intercept age of 1914 ± 26 Ma and a lower intercept at −5 ± 380 Ma. By analogy with sample Ch 020901 and in view of the magmatic origin of the

Table 3
Zircon morphology and isotopic data from single grain evaporation of metamorphic zircons from high-grade mafic dykes and pegmatoid melt of the Hengshan gneiss terrain, North China Craton

Sample number	Zircon colour and morphology	Grain#	Mass scans[a]	Evaporation temperature (°C)	Mean $^{207}Pb/^{206}Pb$ ratio[b] and $2\sigma_m$ error	$^{207}Pb/^{206}Pb$ age and $2\sigma_m$ error
Ch 980871	Clear to pink, ball-round, multifaceted	1[c]	75	1610	0.115064 ± 45	1880.9 ± 0.7
		2[c]	70	1612	0.115088 ± 46	1881.3 ± 0.7
		3[c]	62	1610	0.115071 ± 47	1881.0 ± 0.7
		4[c]	238	1604	0.115101 ± 22	1881.5 ± 0.3
Mean of four grains		1–4	445		0.115089 ± 17	**1881.3 ± 0.4**[d]
Ch 990839	Clear to light grey, long-prismatic, idiomorphic	1	89	1598	0.113482 ± 118	1855.9 ± 1.9
		2	107	1597	0.113512 ± 71	1856.4 ± 1.1
		3	107	1599	0.113488 ± 44	1856.0 ± 0.7
		4	105	1598	0.113503 ± 39	1856.2 ± 0.6
Mean of four grains		1–4	408		0.113497 ± 35	**1856.1 ± 0.6**
Ch 990848	Clear to light grey, ball-round, multifaceted	1[c]	80	1602	0.115369 ± 43	1885.7 ± 0.7
		2[c]	78	1600	0.115308 ± 47	1884.7 ± 0.7
		3[c]	83	1603	0.115331 ± 48	1885.1 ± 0.8
		4[c]	119	1606	0.115354 ± 30	1885.4 ± 0.5
		5[c]	105	1601	0.115348 ± 41	1885.3 ± 0.6
		6[c]	125	1603	0.115320 ± 26	1884.9 ± 0.4
Mean of six grains		1–6	590		0.115367 ± 16	**1885.6 ± 0.4**[d]
Ch 990853	Clear, oval to near-spherical, multifaceted	1[c]	107	1600	0.113731 ± 37	1859.9 ± 0.6
		2[c]	109	1601	0.113720 ± 77	1859.7 ± 1.2
		3[c]	107	1606	0.113707 ± 44	1859.5 ± 0.7
		4[c]	105	1599	0.113722 ± 39	1859.7 ± 0.6
Mean of four grains		1–4	428		0.113720 ± 30	**1859.7 ± 0.5**
Ch 990886	Clear, near-spherical, multifaceted	1[c]	123	1603	0.113482 ± 118	1855.9 ± 1.9
		2[c]	185	1600	0.113512 ± 71	1856.4 ± 1.1
		3[c]	77	1605	0.113488 ± 44	1856.0 ± 0.7
		4[c]	105	1602	0.113503 ± 39	1856.2 ± 0.6
Mean of four grains		1–4	490		0.113497 ± 35	**1850.9 ± 0.4**

[a] Number of $^{207}Pb/^{206}Pb$ ratios evaluated for age assessment.
[b] Observed mean ratio corrected for non-radiogenic Pb where necessary. Errors based on uncertainties in counting statistics.
[c] Errors of combined mean ages (bold font) are based on reproducibility of internal standard at 0.000027 (2σ).
[d] Grain fractions of three to four metamorphic grains each, evaporated together.

zircons we interpret this age to approximate the time of igneous emplacement of the gabbroic dyke. One grain is considerably older with a $^{207}Pb/^{206}Pb$ minimum age of 2469 ± 8 Ma (Fig. 7b), and this again is interpreted as a xenocryst, probably inherited from the basement into which the dyke was emplaced. This age also corresponds well with zircon ages reported for the Hengshan gneisses in the Large Stone and Great Wall Valleys (Kröner et al., 2005a,b).

Excellent agreement in the magmatic crystallization ages for the above two samples leaves little doubt that the Hengshan mafic dykes were emplaced at ~1915 Ma, much later than previously considered, and only shortly before being subjected to high-grade metamorphism (Kröner et al., 2005a). Since the numerous dykes occupy an area much larger than the Hengshan Complex they define a genuine dyke swarm and signify considerable crustal extension prior to the Lüliang orogeny. The tectonic implications will be discussed below.

7.2. *Metamorphic ages and late granite gneiss*

Sample MO68 contains three generations of symplectite, and its mineral composition was described by Zhao et al. (2001b) who also determined peak *P–T* conditions of 13.5–15.5 kbar and 770–840 °C for this sample. The zircon population consists predominantly of oval to spherical, multifaceted grains with well-developed sector zoning (Fig. 6) that are interpreted as metamorphic in view of their similarity with published CL-images of metamorphic zircons elsewhere (e.g. Vavra et al., 1999; Corfu et al., 2003) and because of low Th/U ratios (Bingen et al., 2004, and references cited therein). Five grains were analyzed on the Beijing SHRIMP and produced a near-concordant cluster of data points with a mean $^{207}Pb/^{206}Pb$ age of 1850 ± 3 Ma (Table 1; Fig. 8a), reflecting zircon growth at or close to the peak of HP-metamorphism.

The zircons in sample HG-2 range from weakly elongate crystals with rounded terminations to more equidimensional grains with multifaceted surfaces (Fig. 6). A large number of zircons were analyzed on SHRIMP II in Perth, and the analytical data are listed in Table 2 and are plotted in the concordia diagram of Fig. 8b. Most analyses are concordant or near-concordant, and eight further analyses are significantly discordant but define a linear arrangement (Fig. 8b) that, if regressed together with the concordant or near-concordant data (MSWD = 3.4), yields an upper intercept age of 1867 ± 23 Ma. This is the best estimate for the timing of metamorphic zircon formation in this sample.

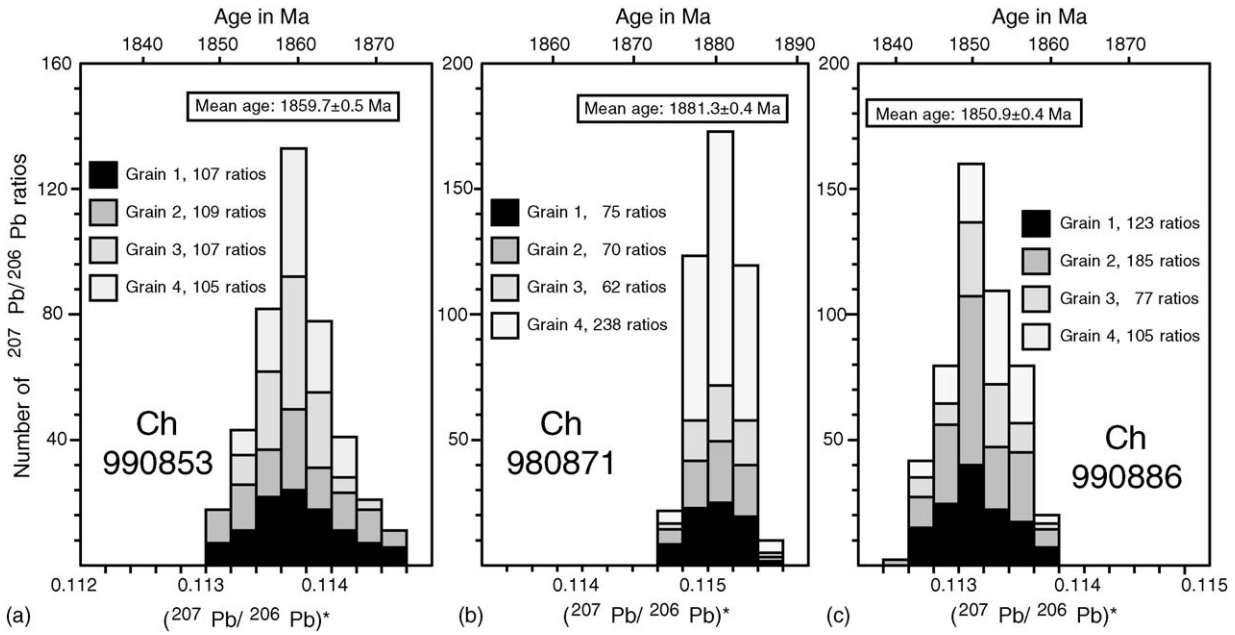

Fig. 9. Histograms showing distribution of radiogenic lead isotope ratios derived from evaporation of small metamorphic zircon fractions of three to four grains each from two gabbroic dyke samples (HP mafic granulites), Hengshan Complex. Errors are 2-sigma (mean). (a) Spectrum for four grain fractions from sample Ch 990853, integrated from 428 ratios. (b) Spectrum for four grain fractions from sample Ch 980871, integrated from 445 ratios. (c) Spectrum for four grain fractions from sample Ch 990886, integrated from 490 ratios.

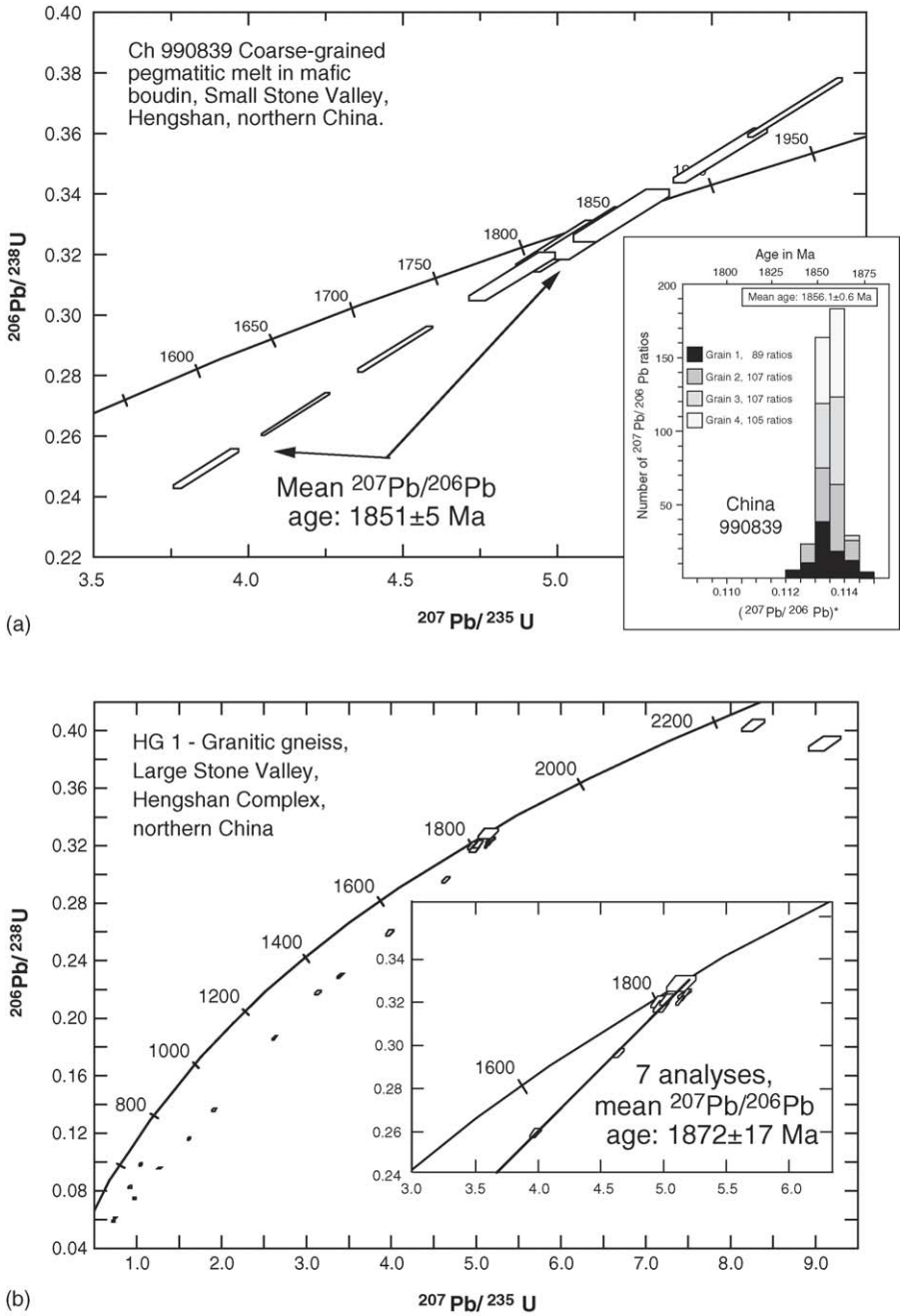

Fig. 10. Concordia diagrams showing SHRIMP II data for spot analyses from Palaeoproterozoic magmatic zircons in granitoid rocks from the Hengshan Complex. For locations see Fig. 2, uncertainties as in Fig. 7a. (a) Pegmatoid melt patch sample Ch 990839, Small Stone Valley. Inset shows histogram for four single magmatic grains from same sample, integrated from 408 ratios. (b) Granitic gneiss sample HG-1, gorge of Dashiyu River, lower Large Stone Valley. Inset shows enlargement of grains near upper concordia intercept.

One further discordant grain is significantly older at 2011 ± 105 Ma (Table 2; Fig. 8b) and is interpreted as a xenocryst.

The zircon population of dyke sample Ch 990853 exclusively consists of clear, oval to spherical, multi-faceted grains with high reflectivity, typical of metamorphic growth (Fig. 6). Four grain fractions of three to four zircons each were evaporated individually and yielded identical $^{207}Pb/^{206}Pb$ ratios, providing a combined mean age of 1859.7 ± 0.5 Ma (Table 3; Fig. 9a). This is

identical to the above SHRIMP ages and again reflects zircon growth at or near the peak of HP-metamorphism.

Sample Ch 980871 also exclusively contains ball-shaped, multifaceted and metamorphic zircons (Fig. 6). Four grain fractions of three to four zircons each were evaporated and produced identical results with a mean $^{207}Pb/^{206}Pb$ age of 1881.3 ± 0.4 Ma (Table 3; Fig. 9b). This age is significantly older than those reported above and may either mean that the peak of metamorphism was diachronous in this region or that the zircons contained small cores of inherited older grains, perhaps trapped during dyke emplacement at ~1915 Ma. We have indeed identified a few ball-shaped grains with cores in this sample (Fig. 6) and therefore favour the second alternative, i.e. inheritance, and suggest that the above "age" reflects a mixture of metamorphic and older components and will not be considered further. However, Zhao et al. (2002a) reported a concordant SHRIMP mean zircon age of 1875 ± 43 Ma for metamorphic zircon grains and rims in a trondhjemitic gneiss of the Fuping complex.

The zircons in sample Ch 990886 are again almost exclusively oval to spherical, clear, multifaceted, and with high reflectivity, and display the characteristic sector zoning (Fig. 6). Four grain fractions of three to four zircons each were evaporated individually, and the results can be combined to a mean $^{207}Pb/^{206}Pb$ age of 1850.9 ± 0.4 Ma (Table 3; Fig. 9c) which, as in the previous samples, we interpret to reflect the time of peak metamorphism.

There are also spectacular examples of large gabbroic boudins in Small Stone Valley containing coarse-grained pegmatoid melt patches (Fig. 6) that probably formed during isothermal decompression shortly after the peak of HP-metamorphism. Sample Ch 990839 (Fig. 2) comes from one of these irregular patches and contains clear, near-euhedral, long-prismatic, magmatic zircons with only slight rounding at their terminations. Nine grains were analyzed on SHRIMP II in Perth and produced remarkably well-aligned analyses three of which are concordant, two are reversely discordant and four are discordant (Table 1; Fig. 10a). Regression of all data suggests recent Pb-loss and internal redistribution of U (Williams et al., 1984) and yields an upper concordia intercept age of 1851 ± 5 Ma (Fig. 10a). Evaporation of four small grain fractions of three to four metamorphic grains each yielded identical results that combine to give a mean $^{207}Pb/^{206}Pb$ age of 1856.1 ± 0.6 Ma (Table 3; Fig. 10a, inset). We consider this to most precisely reflect the melting event associated with post-peak decompression.

Lastly, we report zircon age data for the youngest yet reported granitoid rock in the Hengshan Complex. This is a well-foliated granitic gneiss (HG-1), interlayered with the more migmatitic TTG-gneisses in the deep gorge of the Dashiyu River, close to sample HG-2 (Fig. 2). The zircons are clear to light brown in colour with a multifaceted round to ovoid shape. Many grains are broken, and most contain numerous fine cracks. Twenty-two grains from the >135 μm fraction were analyzed on SHRIMP II in Perth and produced highly variable data (Table 2). Seven data points are concordant or near-concordant, and their mean $^{207}Pb/^{206}Pb$ age is 1872 ± 17 Ma (Fig. 10b, inset). Thirteen points are variably discordant but define a linear array suggesting Pb-loss in recent times. These data only provide a minimum age assessment and are not further considered here. Two discordant analyses are considerably older at 2323 ± 18 and 2525 ± 24 Ma ($^{207}Pb/^{206}Pb$ minimum ages; see Table 2) and are interpreted as xenocrysts. The important implication of the age of ~1872 Ma is that the host granitic gneiss displays the same foliation and structural–metamorphic history as the other Hengshan gneisses and, by implication, this means that the main deformation and associated high-grade metamorphism in the Hengshan Complex must be younger than 1872 ± 17 Ma.

8. Conclusions

Our age data indicate that a mafic dyke swarm intruded late Archaean to Palaeoproterozoic granitoid gneisses of the Hengshan Complex at ~1915 Ma during a major crustal extension event that predated the collision of the Eastern and Western blocks to form the Trans-North China orogen. It may well be possible that these two blocks were part of a single continental mass in the late Archaean and early Palaoproterozoic and only separated during the above extension event. However, no typical features of continental separation such as alkaline complexes, bimodal volcanism, rift or continental margin deposits or remnants of oceanic crust have been identified in the Hengshan. We therefore speculate that mafic dyke emplacement may reflect extension and an unsuccessful attempt to break apart a component of the NCC at ~1915 Ma. Subsequent shortening resulted in significant crustal thickening during which the Hengshan Complex was transferred into the lower crust, acquired its ductile fabric and experienced high-grade metamorphism. This structural–metamorphic event is bracketed between 1872 ± 17 Ma (emplacement of youngest granite) and ~1848 Ma (decompression event in mafic dykes), and is similar to ages derived from SHRIMP-analyses of metamorphic zircons in the nearby Fuping complex (Zhao et al., 2002a).

Therefore, our age data show beyond reasonable doubt that the main tectono-metamorphic event in the Hengshan Complex was late Palaeoproterozoic and not Archaean in age. This conclusion is in agreement with structural and age studies in the gneissic terrain of the Zanhuang Mts. to the southeast of our study area where the most intense deformation occurred between ca. 1870 and 1826 Ma (Wang et al., 2003). Slightly younger metamorphic ages between 1825 and 1802 Ma as recorded in high-grade terrains to the east and north of the Hengshan Complex (Zhao et al., 2002a; Guo et al., 2005) may reflect differences in the collision–accretion history of these terrains within the Central Zone of the NCC.

Our data do not support models of late Archaean cratonization in northern China (Li et al., 2000a,b; Kusky and Li, 2003) but reflect extensive Palaeoproterozoic tectonism and metamorphism, probably related to amalgamation of several Archaean crustal domains. Thus, the Trans-North China orogeny, generally known as the Lüliang orogeny in the Chinese literature, probably was one of the most important events in the history of the NCC (Zhao, 1993; Zhao et al., 2002b, 2005), welding together older domains and similar to the Trans-Hudson orogeny of the Canadian shield (Hoffman, 1988, 1990; Lucas et al., 1996).

Acknowledgements

This contribution resulted from collaboration between the Universities of Mainz, Peking, Potsdam, Curtin, Hong Kong, the Chinese Academy of Geological Sciences and the Chinese Academy of Sciences (formerly Academia Sinica) and was funded by the German Science Foundation (DFG, grant Kr 590/67 to A.K.), the National Natural Science Foundation of China (grant nos. 49832030, 49772143 and 49572140 to Li Jianghai, No. 40429001 to G.C. Zhao and No. 40420120135 to S.W.L.), the German Academic Exchange Service (DAAD), Hong Kong RGC grants 7055/03P, 7048/03P and 7058/04P to M.S., and Australian Research Council Grant A39532446 to S.A.W. A.K. acknowledges mass spectrometer analytical facilities in the Max-Planck-Institut für Chemie in Mainz. Some of the zircon analyses were carried out on the Sensitive High Resolution Ion Microprobe mass spectrometer (SHRIMP II) operated by a consortium consisting of Curtin University of Technology, the Geological Survey of Western Australia and the University of Western Australia with the support of the Australian Research Council. We appreciate the advice of A. Kennedy during SHRIMP analysis. Additional analyses were performed on the SHRIMP II ion microprobe of the Chinese Academy of Geological Sciences, Beijing. We appreciate discussions with Li Jinghai, Zhai Mingguo and Tim Kusky and thorough reviews by Urs Schärer and an anonymous reviewer.

References

Bai, J., 1986. The Precambrian crustal evolution of the Wutaishan area. In: Bai, J. (Ed.), The Early Precambrian Geology of Wutaishan. Tianjin Science and Technology Press, Tianjin, pp. 376–383 (in Chinese).

Bingen, B., Austrheim, H., Whitehouse, M., Davis, W.J., 2004. Trace element signature and U–Pb geochronology of eclogite-facies zircon, Bergen Arcs Caledonides of W Norway. Contrib. Miner. Petrol. 147, 671–683.

Chang, X.Y., Zhu, B.Q., Fan, S.K., Xie, G.H., 1994. High abnormal $\varepsilon_{Nd(T)}$ value and its possible explanation on Archean mantle of northern Shanxi Province. Chin. Sci. Bull. 39, 1351–1355.

Chang, X.Y., Chen, Y.D., Zhu, B.Q., 1999. U–Pb zircon isotope age of metabasites from Hengshan grey gneiss. Acta Min. Sin. 19, 263–266 (in Chinese with English abstract).

Chen, M.Y., Li, S.X., 1996. Metamorphic evolution of granulites in Eastern Hebei. Acta Petrol. Sin. 12, 343–357 (in Chinese with English abstract).

Cherniak, D.J., Hanchar, J.M., Watson, E.B., 1997. Diffusion of tetravalent cations in zircon. Contrib. Miner. Petrol. 127, 383–390.

Claoué-Long, J.C., Sobolev, N.V., Shatsky, V.S., Sobolev, A.V., 1991. Zircon response to diamond-pressure metamorphism in the Kokchetav massif, USSR. Geology 19, 710–713.

Claoué-Long, J.C., Compston, W., Roberts, J., Fanning, C.M., 1995. Two Carboniferous ages: a comparison of SHRIMP zircon dating with conventional zircon ages and $^{40}Ar/^{39}Ar$ analysis. In: Geochronology time scales and global stratigraphic correlation. SEPM Special Publication 54, 3–20.

Cocherie, A., Guerrot, C., Rossi, P.H., 1992. Single-zircon dating by stepwise Pb evaporation: comparison with other geochronological techniques applied to the Hercynian granites of Corsica, France. Chem. Geol. 101, 131–141.

Corfu, F., Hanchar, M., Hoskin, P.W.O., Kinny, P., 2003. Atlas of zircon textures. Rev. Miner. Geochem. 53, 469–500.

Cumming, G.L., Richards, J.R., 1975. Ore lead isotope ratios in a continuously changing earth. Earth Planet. Sci. Lett. 28, 155–171.

de Laeter, J.R., Kennedy, A.K., 1998. A double focusing mass spectrometer for geochronology. Int. J. Mass Spectrom. 178, 43–50.

Gebauer, D., Tilton, G.R., Schertl, H.P., Schreyer, W., 1993. Eocene/oligocene ultrahigh-pressure (UHP)-metamorphism in the Dora Maira Massif (Western Alps) and its geodynamic implications. Terra Abstracts, Supplement to Terra Nova, vol. 5, pp. 10–11.

Geisler, T., Rashwan, A.A., Rahn, M.K.W., Poller, U., Zwingmann, H., Pidgeon, R.T., Schleicher, H., Tomaschek, F., 2003. Low-temperatire hydrothermal alteration of natural metamict zircons from the Eastern Desert, Egypt. Miner. Mag. 67, 485–508.

Goodwin, A.M., 1991. Precambrian Geology—The Dynamic Evolution of the Continental Crust. Academic Press, Toronto, p. 666.

Guan, H., Sun, M., Wilde, S.A., Zhou, X.H., Zhai, M.G., 2002. SHRIMP U–Pb zircon geochronology of the Fuping Complex: implications for formation and assembly of the North China craton. Precambrian Res. 113, 1–18.

Guo, J.H., Zhai, M.G., Li, Y., 1996. Isotopic ages and their tectonic significance of metamorphic rocks from middle part of the early Precambrian granulite belt North China craton. In: Qian, X.L.,

Wang, R.M. (Eds.), Geological Evolution of the Granulite Terranes in the North Part of the North China Craton. Seismological Press, Beijing, pp. 120–129 (in Chinese with English abstract).

Guo, J.H., Wang, S.S., Sang, H.Q., Zhai, M.G., 2001. ^{40}Ar–^{39}Ar age spectra of garnet porphyroblast: implications for metamorphic age of high-pressure granulite in the North China craton. Acta Petrol. Sin. 17, 436–442 (in Chinese with English abstract).

Guo, J.H., O'Brien, P.J., Zhai, M.G., 2002. High-pressure granulites in the Sangan area, North China Craton: metamorphic evolution *P–T* paths and geotectonic significance. J. Metam. Geol. 20, 741–756.

Guo, J.H., Sun, M., Chen, F.K., Zhai, M.G., 2005. Sm–Nd and SHRIMP U–Pb zircon geochronology of high-pressure granulites in the Sanggan area North China Craton: timing of Paleoproterozoic continental collision. J. Asian Earth Sci. 24, 629–642.

Halls, H.C., Li, J.H., Davis, D., Hou, G.T., Zhang, B.X., Qian, X.L., 2000. A precisely dated Proterozoic palaeomagnetic pole from the North China Craton, and its relevance to palaeocontinental reconstruction. Geophys. J. Int. 143, 185–203.

Hoffman, P.F., 1988. United plates of America, the birth of a craton: early Proterozoic assembly and growth of Laurentia. Ann. Rev. Earth Planet. Sci. 16, 543–603.

Hoffman, P.F., 1990. Dynamics of the tectonic assembly of northeast Laurentia in geon-18 (1.9–1.8-Ga). Geosci. Canada 17, 222–226.

Hoskin, P.W., Black, L.P., 2000. Metamorphic zircon formation by solid-state recrystallization of protolith igneous zircon. J. Metam. Geol. 18, 423–439.

Hou, G., Liu, Y., Li, J., 2006. Evidence for ~1.8 Ga extension of the eastern block of the North China craton from SHRIMP U–Pb dating of mafic dyke swarms in Shandong Province. J. Asian Earth Sci., 27, in press.

Huang, J.Q., 1977. The basic outline of China tectonics. Acta Geol. Sin. 52, 117–135.

Jaeckel, P., Kröner, A., Kamo, S.L., Brandl, G., Wendt, J.I., 1997. Late Archaean to early Proterozoic granitoid magmatism and high-grade metamorphism in the central Limpopo belt South Africa. J. Geol. Soc. Lond. 154, 25–44.

Jin, W., Li, S.X., 1996. *P–T–t* path and crustal thermodynamic model of late Archaean-early Proterozoic high-grade metamorphic terrain in North China. Acta Petrol. Sin. 12, 208–221.

Karabinos, P., 1997. An evaluation of the single-grain zircon evaporation method in highly discordant samples. Geochim. Cosmochim. Acta 61, 2467–2474.

Kelly, N.M., Harley, S.L., 2005. An integrated microtextural and chemical approach to zircon geochronology: refining the Archaean history of the Napier Complex, east Antarctica. Contrib. Miner. Petrol. 149, 57–84.

Kinny, P.D., 1986. 3820 Ma zircons from a tonalitic Amitsoq gneiss in the Godthab district of southern West Greenland. Earth Planet. Sci. Lett. 79, 337–347.

Kröner, A., Byerly, G.R., Lowe, D.R., 1991. Chronology of early Archean granite-greenstone evolution in the Barberton Mountain Land, South Africa, based on precise dating by single zircon evaporation. Earth Planet. Sci. Lett. 103, 41–54.

Kröner, A., Jaeckel, P., Williams, I.S., 1994. Pb-loss patterns in zircons from a high-grade metamorphic terrain as revealed by different dating methods: U–Pb and Pb–Pb ages for igneous and metamorphic zircons from northern Sri Lanka. Precambrian Res. 66, 151–181.

Kröner, A., Hegner, E., 1998. Geochemistry, single zircon ages and Sm–Nd systematics of granitoid rocks from the Góry Sowie (Owl) Mts., Polish West Sudetes: evidence for early Palaeozoic arc-related plutonism. J. Geol. Soc. Lond. 155, 711–724.

Kröner, A., Willner, A.P., 1998. Time of formation and peak of HP-HT metamorphism for quartz-feldspar rocks in the central Erzgebirge, Saxony, Germany. Contrib. Miner. Petrol. 132, 1–20.

Kröner, A., Jaeckel, P., Reischmann, T., Kroner, U., 1998. Further evidence for an early Carboniferous (~340 Ma) age of high-grade metamorphism in the Saxonian Granulite Complex. Geol. Rundschau 86, 751–766.

Kröner, A., Jaeckel, P., Brandl, G., Nemchin, A.A., Pidgeon, R.T., 1999. Single zircon ages for granitoid gneisses in the Central Zone of the Limpopo belt, southern Africa, and geodynamic significance. Precambrian Res. 93, 299–337.

Kröner, A., O'Brien, P.J., Nemchin, A.A., Pidgeon, R.T., 2000. Zircon ages of high pressure granulites from S Bohemia, Czech Republic, and their bearing on the connection between Variscan high temperature metamorphism at high and low pressures. Contrib. Miner. Petrol. 138, 127–142.

Kröner, A., Wilde, S.A., Li, J.H., Wang, K.Y., 2005a. Age and evolution of a late Archean to early Palaeoproterozoic upper to lower crustal section in the Wutaishan/Hengshan/Fuping terrain of northern China. J. Asian Earth Sci. 24, 577–596.

Kröner, A., Li, J.H., Wilde, S.H., O'Brien, P.J., Walte, N.P., Passchier, C.P., 2005b. Zircon ages and evolution of a late Archean to Paleoproterozoic lower crustal section in the Hengshan terrain of northern China. Acta Geol. Sin. 79, 605–629.

Krogh, T.E., 1993. High precision U–Pb ages for granulite metamorphism and deformation in the Archean Kapuskasingm structural zone Ontario: implications for structure and development of the lower crust. Earth Planet. Sci. Lett. 119, 1–18.

Kusky, T.M., Li, J.H., 2003. Paleoproterozoic tectonic evolution of the North China craton. J. Asian Earth Sci. 22, 23–40.

Lee, J.K.W., Williams, I.S., Ellis, D.J., 1997. Pb U and Th diffusion in natural zircon. Nature 390, 159–161.

Li, Z.L., 1993. Metamorphic *P–T–t* path of the Archaean rocks in the eastern Shandong Province and its implications. Shandong Geol. 9, 31–41 (in Chinese).

Li, J.H., Qian, X.L., 1991. A study of Longquanguan shear zone in the northern part of the Taihang Mountain. Shanxi Geol. 6, 17–29 (in Chinese).

Li, J.H., Qian, X.L., 1994. The Early Precambrian Crustal Evolution of Hengshan Metamorphic Terrain North China Craton. Shanxi Science and Technology Press, p. 124 (in Chinese with extended English abstract).

Li, J.H., Zhai, M.G., Li, Y.G., 1998a. Discovery of Neoarchean high-pressure granulites in Luanping-Chengde area, Northern Hebei, and their tectonic-geological implications. Acta Petrol. Sin. 14, 34–41.

Li, J.H., Zhai, M.G., Qian, X.G., 1998b. The geological occurrence, regional tectonic setting and exhumation of late Archean high-pressure granulite within the high-grade metamorphic terrains, north to central portion of North China Craton. Acta Petrol. Sin. 14, 176–189.

Li, J.H., Zhai, M.G., Qian, X.L., Guo, J.H., Wang, G.Y., Yan, Y.H., Li, Y.G., 1998. The geological occurrence, regional tectonic setting and exhumation of late Archean high-pressure granulite within the high-grade metamorphic terrains, north to central portion of North China Craton. Acta Petrol. Sin. 14, 176–189 (in Chinese with English abstract).

Li, J.H., Qian, X.L., Huang, X.N., Liu, S.W., 2000a. The tectonic framework of the basement of North China craton and its implication for the early Precambrian cratonization. Acta Petrol. Sin. 16, 1–10.

Li, J.H., Kröner, A., Qian, X.L., O'Brien, P., 2000b. The tectonic evolution of an early Precambrian high-pressure granulite belt in the North China craton. Acta Geol. Sin. 74, 246–256.

Li, J.H., Kröner, A., Huang, X.N., Zhang, Z.Q., 2002. The discovery of the Neoarchean mafic dyke swarm in Hengshan and reinterpretation of the previous "Wutai greenstone belt". Sci. Chin. Ser. D 45, 680–690.

Liu, D., Page, Y., Compston, R.W., Wu, W.J., 1985. U–Pb zircon geochronology of late Archean metamorphic rocks in the Taihangshan-Wutaishan area North China. Precambrian Res. 27, 85–109.

Liu, D.Y., Shen, Q.H., Zhang, Z.Q., Jahn, B.M., Auvray, B., 1990. Archean crustal evolution in China: U–Pb geochronology of the Qianxi Complex. Precambrian Res. 48, 223–244.

Liu, S.W., 1996. P-T path of the granulites in the Fuping Complex. Geol. J. Chin. Univ. 2, 75–84 (in Chinese with English abstract).

Liu, S.W., Li, J.H., Pan, Y.M., Zhang, J., Li, Q.G., 2002. An Archean continental block in the Taihangshan and Hengshan regions: constraints from geochronology and geochemistry. Prog. Nat. Sci. 12, 568–576.

Liu, S.W., Pan, Y.M., Xie, Q.L., Zhang, J., Li, Q.G., 2004. Archean geodynamics in the Central Zone, North China craton: constraints from geochemistry of two contrasting series of granitoids in the Fuping Hengshan and Wutaishan complexes. Precambrian Res. 130, 229–249.

Liu, X.S., Jin, W., Li, S.X., Xu, X.C., 1993. Two types of Precambrian high-grade metamorphism, Inner Mongolia, China. J. Metam. Geol. 11, 499–510.

Lu, L.Z., Jin, S.Q., 1993. *P–T–t* paths and tectonic history of an early Precambrian granulite facies terrane, Jining district, southeastern Inner Mongolia, China. J. Metam. Geol. 11, 483–498.

Lucas, S.B., Stern, R.A., Syme, E.C., Reilly, B.A., Thomas, D.J., 1996. Interaoceanic tectonics and the development of continental crust: 1.92–1.84 Ga evolution of the Flinn Flon Belt, Canada. Geol. Soc. Am. Bull. 108, 602–629.

Ludwig, K.R., 2003. User's Manual for Isoplot/EX Version 3.00. A Geochronological Toolkit for Microsoft Excel, vol. 4. Berkeley Geochronology Center Special Publication, 71 pp.

Ma, X.Y., Bai, J., Suo, S.T., Lao, Q.Y., Zhang, J.S., 1987. The Precambrian tectonic framework and the research method in China. Geol. Publ. House, Beijing (in Chinese with English abstract).

Ma, J., Wang, R.M., 1994. Reviews of garnet-clinopyroxene geothermometers and geobarometers with their application to granulites: comparision of *P–T* evoution of the Miyun (Zunhua) and Xuanhua granulites. In: Qian, X.L., Wang, R.M. (Eds.), Geological Evolution of the Granulite Terrain in the Northern Part of the North China Craton. Seismological Press, Beijing, pp. 71–88.

Mezger, K., Krogstad, E.J., 1997. Interpretation of discordant U–Pb zircon ages: an evaluation. J. Metam. Geol. 15, 127–140.

Möller, A., O'Brien, P.J., Kennedy, A., Kröner, A., 2002. Polyphase zircon in ultrahigh-temperature granulites (Rogaland SW Norway): constraints for Pb diffusion in zircon. J. Metam. Geol. 20, 727–740.

Myers, J.S., 1978. Formation of banded gneisses by deformation of igneous rocks. Precambrian Res. 6, 43–64.

Nelson, D.R., 1996. Compilation of SHRIMP U–Pb zircon geochronology data. Geol. Surv. Western Australia, 189 (Record 1997/2).

O'Brien, P.J., Walte, N., Li, J.H., 2005. The petrology of two distinct Paleoproterozoic granulite types in the Hengshan Mts., North China craton, and tectonic implications. J. Asian Earth Sci. 24, 615–627.

Peng, P., Zhai M., Zhang, H., Guo, J., 2005. Geochronological constraints on early Proterozoic evolution of the North China Block: SHRIMP zircon ages of different types of dykes. Int. Geol. Rev., 47, in press.

Pidgeon, R.T., Nemchin, A.A., Hitchen, G.J., 2000. Fir-tree and nebulously zoned zircons from granulite facies rocks: evidence for zircon growth and interaction with metamorphic fluids. Goldschmidt 2000. J. Conf. Abstr. 5, 798.

Schertl, H.P., Schreyer, W., 1995. Mineral inclusions in heavy minerals of the ultrahigh-pressure metamorphic rocks of the Dora-Maira massif and their bearing on the relative timing of the petrological events. In: Basu, A., Hart, S.R. (Eds.), Earth Processes: Reading the Isotopic Code. American Geophysical Union, Monograph Series, vol. 95, pp. 331–342.

Silver, L.T., 1969. A geochronological investigation of the anorthosite complex, Adirondack Mountains New York. In: Isachsen, Y.W. (Ed.), Origin of Anorthosite and Related Rocks. New York Museum and Science Service, Memoir 18, pp. 57–82.

Sobolev, N.V., Shatsky, V.S., Vavilov, M.A., Goryaynov, S.V., 1992. A coesite inclusion in zircon from diamond-containing gneiss of the Kokchetav massif: the first find of coesite in metamorphic rocks of the USSR. Trans. Russ. Acad. Sci. (Earth Science Section) 322, 123–127.

Stern, R.A., 1997. The GSC sensitive high resolution ion microprobe (SHRIMP): analytical techniques of zircon U–Th–Pb age determinations and performance evaluation. In: Radiogenic Age and Isotope Studies, Geol. Surv., Canada, Report 10, Current Research, p. F1-31.

Tian, Y.Q., Liang, Y.F., Fan Sikun, Zhu, B.Q., Chen, Y.W., 1992. Geochronology of the Hengshan Complex in special reference to Nd isotopic evolution. Geochimica 9, 255–264 (in Chinese with English abstract).

Tian, Y.Q., Ma, Z.H., Yu, K.R., Liu, Z.H., Peng, Q.M., 1996. The early Precambrian geology of Wutai-Hengshan Mts., Shanxi, China. In: Field Trip Guide T315 30th International Geological Congress, Beijing, China. Geological Publishing House, Beijing, 52 pp.

Vavra, G., 1990. On the kinematics of zircon growth and its petrogenetic significance: a cathodoluminescence study. Contrib. Miner. Petrol. 106, 90–99.

Vavra, G., Schmid, R., Gebauer, D., 1999. Internal morphology, habit and U–Th–Pb microanalysis of amphibolite-to-granulite facies zircons: geochronology of the Ivrea Zone (Southern Alps). Contrib. Miner. Petrol. 134, 380–404.

Wang, H., Mo, X., 1995. An outline of the tectonic evolution of China. Episodes 18, 6–16.

Wang, R.M., Chen, Z.Z., Chen, F., 1991. Grey gneisses and high-pressure granulite enclaves in the Hengshan area and their geological implications. Acta Petrol. Sin. 7, 36–46 (in Chinese with English abstract).

Wang, Y.J., Fan, W.M., Zhang, Y., Guo, F., 2003. Structural evolution and $^{40}Ar/^{39}Ar$ dating of the Zanhuang metamorphic domain in the North China Craton: constraints on Palaeoproterozoic tectonothermal overprinting. Precambrian Res. 122, 159–182.

Wang, Z., Wilde, S.A., Wang, K., Yu, L., 2004a. A MORB-arc basalt-adakite association in the 2.5 Ga Wutai greenstone belt: late Archean magmatism and crustal growth in the North China Craton. Precambrian Res. 131, 323–343.

Wang, Y., Fan, W., Zhang, Y., Guo, F., Zhang, H., Peng, T., 2004b. Geochemical $^{40}Ar/^{39}Ar$ geochronological and Sr-Nd isotopic constraints on the origin of Paleoproterozoic mafic dikes from the southern Taihuang Mountains and implications for the ca. 1800 Ma event of the North China craton. Precambrian Res. 135, 55–77.

Wilde, S.A., Cawood, P., Wang, K.Y., Nemchin, A., 1997. The relationship and timing of granitoid evolution with respect to felsic volcanism in the Wutai Complex, North China Craton. Proceedings of the 30th International Geological Congress, Beijing. Precambrian Geol. Metamorph. Petrol. 17, 75–88.

Wilde, S.A., Cawood, P.A., Wang, K.Y., Nemchin, A., 1998. SHRIMP U–Pb zircon dating of granites and gneisses in the Taihangshan-Wutaishan area: implications for the timing of crustal growth in the North China craton. Chin. Sci. Bull. 43, 144–145.

Wilde, S.A., Cawood, P.A., Wang, K.Y., Nemchin, A., Zhao, G.C., 2004. Determining Precambrian crustal evolution in China: a case-study from Wutaishan, Shanxi Province, demonstrating the application of precise SHRIMP U–Pb geochronology. In: Malpas, J., Fletcher, C.J.N., Ali, J.R., Aitchison, J.C. (Eds.), Aspects of the Tectonic Evolution of China, Special Publication, vol. 226. Geological Society of London, pp. 5–25.

Williams, I.S., 1998. U–Th–Pb geochronology by ion microprobe. In: McKibben, M.A., Shanks III, W.C., Ridley, W.I. (Eds.), Applications of Microanalytical Techniques to Understanding Mineralizing Processes. Rev. Econ. Geol. 7, 1–35.

Williams, I.S., Compston, W., Black, L.P., Ireland, T.R., Foster, J.J., 1984. Unsupported radiogenic Pb in zircon: a cause of anomalously high Pb–Pb U–Pb and Th–Pb ages. Contrib. Miner. Petrol. 88, 322–327.

Zhai, M.G., 1997. Recent advances in the study of granulites from the North China craton. Int. Geol. Rev. 39, 325–341.

Zhai, M.G., Guo, J.H., Li, H.H., Yan, Y.H., Li, Y.G., 1995. Discovery of retrograded eclogites in the Archaean North China Craton. Chin. Sci. Bull. 40, 1590–1594.

Zhai, M.G., Bian, A.G., Zhao, T.P., 2000. The amalgamation of the supercontinent of North China Craton at the end of Neo-Archaean and its breakup during late Palaeoproterozoic and Mesoproterozoic. Sci. Chin. Ser. D 43, 219–232.

Zhai, M.G., Guo, J.H., Yan, Y.H., 1993. Discovery and preliminary study of the Archean high-pressure granulites in the North China. Sci. Chin. 36, 1402–1408.

Zhang, Z.Q., Wu, J.S., Ye, X.J., 1991. Archean metamorphic rocks from the lower Fuping in the Mt. Taihang region, North China: REE geochemistry, Rb–Sr and Sm–Nd ages and implications. Geochimica 2, 118–127 (in Chinese with English abstract).

Zhao, Z.P., 1993. Precambrian Crustal Evolution of the Sinica-Korean Platform. Sciences Press, Beijing (in Chinese).

Zhao, G.C., 2001. Paleoproterozoic assembly of the North China Craton. Geol. Mag. 138, 87–91.

Zhao, G.C., Wilde, S.A., Cawood, P.A., Lu, L.Z., 1998. Thermal evolution of the Archaean basement rocks from the eastern part of the North China Craton and its bearing on tectonic setting. Int. Geol. Rev. 40, 706–721.

Zhao, G.C., Wilde, S.A., Cawood, P.A., Li, L.Z., 1999a. Tectonothermal history of the basement rocks in the western zone of the North China Craton and its tectonic implications. Tectonophysics 310, 37–53.

Zhao, G.C., Wilde, S.A., Cawood, P.A., Lu, L.Z., 1999b. Thermal evolution of two textural types of mafic granulites in the North China Craton: evidence for both mantle plume and collisional tectonics. Geol. Mag. 136, 223–240.

Zhao, G.C., Cawood, P.A., Lu, L.Z., 1999c. Petrology and *P–T* history of the Wutai amphibolites: implications for tectonic evolution of the Wutai Complex. China. Precambrian Res. 93, 181–199.

Zhao, G.C., Cawood, P.A., Wilde, S.A., Lu, L.Z., 2000a. Metamorphism of basement rocks in the Central Zone of the North China Craton: implications for Paleoproterozoic tectonic evolution. Precambrian Res. 103, 55–88.

Zhao, G.C., Wilde, S.A., Cawood, P.A., Lu, L.Z., 2000b. Petrology and *P–T* path of the Fuping mafic granulites: implications for tectonic evolution of the central zone of the North China Craton. J. Metam. Geol. 18, 375–391.

Zhao, G.C., Cawood, P.A., Wilde, S.A., Lu, L.Z., 2001a. High-pressure granulites (retrograded eclogites) from the Hengshan Complex North China Craton: petrology and tectonic implications. J. Petrol. 42, 1141–1170.

Zhao, G.C., Wilde, S.A., Cawood, P.A., Sun, M., 2001b. Archean blocks and their boundaries in the North China Craton: lithological, geochemical, structural and *P–T* path constraints and tectonic evolution. Precambrian Res. 107, 45–73.

Zhao, G.C., Wilde, S.A., Cawood, P.A., Sun, M., 2002a. SHRIMP U–Pb zircon ages of the Fuping Complex: implications for late Archean to Paleoproterozoic accretion and assembly of the North China Craton. Am. J. Sci. 302, 191–226.

Zhao, G.C., Cawood, P.A., Wilde, S.A., Sun, M., 2002b. Review of global 2.1–1.8 Ga orogens: implications for a pre-Rodinia supercontinent. Earth Sci. Rev. 59, 125–162.

Zhao, G.C., Sun, M., Wilde, S.A., Li, S., 2005. Late Archean to Paleoproterozoic evolution of the North China Craton: key issues revisited. Precambrian Res. 136, 177–202.